RSC Advances

PAPER

View Article Online
View Journal | View Issue

Cite this: *RSC Adv.*, 2021, **11**, 35624

Influence of coal treatments on the Ni loading mechanism of Ni-loaded lignite char catalysts

Ronnachai Tipo,[ac] Chatchawan Chaichana,[b] Reiji Noda[d] and Suparin Chaiklangmuang *[cef]

Many kinds of lignite coals have been used as catalyst supporters for preparing the Ni-loaded lignite char catalyst. However, these coals have different properties; especially ash content. The ash in coal affects the mechanism of Ni-loading on the position of the functional group structures in coal. In catalyst preparation, it is interesting that the difference in coal properties might directly influence the mechanism of Ni loading. To prove this point, the coal sample needed to be treated before the catalyst preparation. MM coal (original coal) was treated with acid (HClMM and AceMM coals), alkali (NaMM coal) and alkali followed by acid treatments (NaHClMM and NaAceMM coals). Then, Ni was loaded on the five treated coals by the ion-exchange technique. The Ni-loaded lignite coals were pyrolyzed at 650 °C under a N_2 atmosphere to prepare the Ni-loaded lignite char catalysts. The Ni-loading mechanisms were studied *via* FTIR, XRD, AAS and SEM-EDS analyses. The results showed that the different treatments affected the ash content and the functional groups in the coals. The decreases in the ash contents of HClMM, AceMM, NaHClMM and NaAceMM coals indicated that the exchangeable metallic species were removed by transforming metal-carboxylates into carboxyl groups. The transformations of metal-carboxylates were confirmed by the increased $\Delta\vartheta(COO^-)$ value. For acid treatment, the ion exchange of Ni was controlled by carboxyl groups, while in alkali treatment it occurred through hydroxyl and metal-carboxyl groups. In alkali followed by acid treatment, Ni ions were exchanged with hydroxyl and carboxyl groups. The Ni ion forms, $Ni(NH_3)_6^{2+}$ and/or $Ni(H_2O)_6^{2+}$, appeared on the modified coals. Through pyrolysis, the Ni ion was reduced to Ni metal that was observed in the XRD patterns of the catalysts. The Ni contents of the catalysts were in the range of 16.51–20.07 wt%. The thermal behaviours of the catalysts were presented *via* TGA-DTG.

Received 30th June 2021
Accepted 21st September 2021

DOI: 10.1039/d1ra05046j

rsc.li/rsc-advances

1. Introduction

Lignite has mostly been used as a major fuel in power generation. However, it has caused many environmental problems that are critical global issues, such as climate change, global warming, air pollution and acid rain. Accordingly, several researchers have attempted to find other ways to take advantage of lignite. One of the greatest advantages of lignite is the abundance of oxygen-containing functional groups such as phenolic hydroxyl, carboxyl, ether and carbonyl groups.[1] These oxygen-containing functional groups are able to exchange ions with metal ions and disperse them within the coal matrix.[2] Therefore, lignite has been used as a catalyst support material to prepare noble metal catalysts, particularly Ni-loaded lignite char catalysts.

Several literature reviews report[2–6] that many kinds of lignite coals have been used as a catalyst supporter for preparing Ni-loaded lignite catalysts such as Loy Yang coal, Yollourn coal, Eco coal, Mea Moh coal and Shengli coal. The catalysts were prepared from each of these high-performance lignite coals to produce H_2 in biomass gasification. However, these coals had different properties; especially ash content. Loy Yang, Yollourn and Eco coals showed low ash content in the range of 0.40–4.20 wt% (ref. 2–4) while, Mea Moh coal and Shengli coal showed high ash content in the range of 6.50–25.12 wt%.[5,6] It is well known that the ash content in coal is related to the mineral matter in coal.[7] Most mineral matter in low-rank coal is exchangeable metallic species such as Na^+, K^+, Ca^{2+} and Mg^{2+}. These exchangeable metallic species are associated with the oxygen-containing functional groups.[8]

[a]*Graduate Program in Industrial Chemistry, Faculty of Science, Chiang Mai University, Chiang Mai 50200, Thailand*
[b]*Department of Mechanical Engineering, Faculty of Engineering, Chiang Mai University, Chiang Mai 50200, Thailand*
[c]*Department of Industrial Chemistry, Faculty of Science, Chiang Mai University, Chiang Mai 50200, Thailand. E-mail: suparin.c@cmu.ac.th*
[d]*Department of Environmental Engineering Science, Graduate School of Science and Technology, Gumma University, Gunma 376-8515, Japan*
[e]*Center of Excellence in Materials Science and Technology, Faculty of Science, Chiang Mai University, Chiang Mai, 50200, Thailand*
[f]*Materials Science Research Center, Faculty of Science, Chiang Mai University, Chiang Mai 50200, Thailand*

According to the analysis of the coal treatment literature, it was found that the coal treatment had several methods such as acid treatment, alkali treatment and alkali followed by acid treatment. Each of the methods had a different effect on ash removal in coal. Acid treatment demineralized some minerals in coal such as carbonates, Fe_2O_3, and sulphides; however, it could not leach the clay-bearing minerals.[9] For alkali treatment, alkali solutions such as NaOH could dissolve silica and alumina and other silica-alumina clay-bearing minerals in coal and convert them into sodium silicate and sodium aluminate, which were leached out into the solution.[10] For the alkali followed by acid treatment, the combination of alkali and acid treatments was one of the great methods for ash removal in coal because the acid treatment could dissolve sodalites and sodium-aluminosilicates that were formed after the alkali treatment. Sometimes, mild acid washing also reduced the extra sodium compounds along with acid-soluble minerals in coal.[11]

Previous reports on coal treatment also indicated that the types of leaching reagents affected the properties of coal or carbon materials. For instance, Starck *et al.*[12] reported that the coal treatment with HCl and HF acid solution could remove ash and significantly modify the surface chemistry of lignite, which was able to develop the adsorbent properties of lignite. Ren *et al.*[13] found that coal treatment with HCl significantly decreased the content of metal cation associated with the oxygen-containing functional groups. It led to an increase in Ni-loading and improved the characteristics of the Ni-loaded lignite char catalyst. Radenovic and Malina[14] reported that acetic acid could modify carbon black to adsorb nickel ions from an aqueous solution because acetic acid contained carboxylic functional groups. The affinity of the carboxylic functional groups for metal ions was high. As a result, the adsorption of Ni on carbon black increased. Shah *et al.*[15] reported that the acetic acid treatment could improve the adsorption capacities and selectivity for dibenzothiophene of activated charcoal due to an increase in the surface area, pore size and pore volume. Mukherjee *et al.*[16] found that coal treatment with NaOH solution could remove the ash in coal and improve the cation exchange capacity of coal due to the accumulation of sodium aluminosilicate. Sodium aluminosilicate could entrap water molecules and soluble salt, and sodium ions in NaOH-treated coal were also exchangeable. Feng *et al.*[17] discovered that the elimination of minerals and organic matter in coal by NaOH treatment caused an increase in the macropore volume, which could increase the adsorbed water content. These literature reviews reflected that coal treatment with different chemical reagents not only removed ash in coal but might also affect coal properties, especially the adsorption and cation exchange capacities. Interestingly, the coal treatment might influence the mechanism of the ion exchange of metal ions to prepare Ni-loaded lignite char catalyst. Consequently, it is one of the points considered worthwhile for discussion in this study.

Our previous publications mainly focused on the usage of a novel Ni/char catalyst *via* ion exchange in some applications such as catalytic steam gasification[6,18] and catalytic hydrotreatment[19] on various materials. In terms of catalyst preparation, it is doubtful that the difference in ash content in coal might directly influence the mechanism of the ion exchange of metal ions with oxygen-containing functional groups on coal. A few studies have been conducted on this issue and the results have been unclear.

To prove and understand the influence of the ash content in coal on the mechanism of Ni ion exchange on coal, this work has focused on the influence of coal treatment on the Ni ion-exchange mechanism for the preparation of Ni-loaded lignite char catalyst. Mae Moh coal (MM coal) was represented in this study. MM coal was subjected to acid treatment, alkali treatment and alkali followed by acid treatment; the modified coals were used as catalyst supporters. The leaching reagents, HCl, CH_3COOH and NaOH, were applied in the coal treatments. The treated coals were prepared as Ni-loaded lignite coals by an ion-exchange method, then the Ni-loaded lignite coals were made into Ni-loaded lignite catalysts by pyrolysis at 650 °C under N_2 atmosphere. The ash contents of untreated coal and treated coals were determined using different analytical techniques. Fourier Transform Infrared Spectroscopy (FTIR) analysis was performed as the major technique for investigating the mechanisms of Ni-loaded lignite char catalysts. Moreover, all catalysts in this work were characterized by X-ray Diffraction (XRD), Atomic Absorption Spectroscopy (AAS), SEM-EDS and TGA-DTG analyses to support the investigations.

2. Materials and methods

2.1 Material

The lignite coal was collected from the Mae Moh Mine of the Electricity Generating Authority of Thailand. The coal sample was sieved to provide a particle size of ≤0.25 mm. The coal sample examinations in terms of the proximate, ultimate, calorific value and total sulphur were analysed according to ASTM E870-82, ASTM D3176, ASTM E711-87 and ASTM D3177, respectively. The main chemical composition of MM coal was analysed by X-ray Fluorescence Spectroscopy (XRF), which was done according to ASTM D 4326-13.

2.2 Methods

2.2.1 Chemical coal treatment. MM coal was treated by three different processes for the preparation of Ni-loaded lignite char catalysts: (i) acid treatment, (ii) alkali treatment and (iii) alkali followed by acid treatment. The leaching reagents for coal treatment in this work were hydrochloric acid (ARI Labscan), acetic acid (ARI Labscan) and sodium hydroxide (Carlo Erba). Each of the coal treatment processes used about 25 g of coal sample. All coal treatment processes were conducted under reflux at 95–98 °C. The coal treatment setup for the experiment is shown in Fig. 1. The details of each treatment process are as follows:

(i) Acid treatment; HCl and CH_3COOH solutions were used as leaching agents to treat MM coal. According to our previous research,[20] MM coal was mixed with 0.5 M of the acids. The mixtures were refluxed by stirring for 3 h and then the mixtures were cooled and filtered. The residues were washed with hot

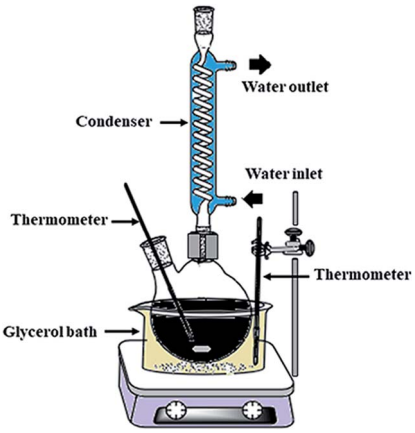

Fig. 1 Experimental setup for coal treatment.

deionized water and dried at 105 °C overnight. The coals treated with HCl and CH_3COOH were labelled HClMM and AceMM, respectively.

(ii) Alkali treatment; the coal sample was mixed with 2.5 M NaOH under reflux for 1 h.[10,21,22] The residue was separated, washed and dried. The alkali-treated coal was called NaMM coal.

(iii) Alkali followed by acid treatment; NaMM coal was continuously treated with HCl and CH_3COOH solutions at 0.5 M and the procedures were similar to process (i). The treated coals were identified as NaHClMM coal and NaAceMM coal, respectively.

After the treatments, the coals were analysed by proximate analysis and the total sulphur content was determined by using standard methods (ASTM D3174 and ASTM D3177, respectively). The percentages of ash removal in the coal treatments were calculated using eqn (1).

$$\text{Ash removal (\%)} = [(W_1 - W_2)/(W_1)] \times 100 \quad (1)$$

where W_1 is the ash content of the original coal (wt%). W_2 is the ash content of the treated coal (wt%).

2.2.2 Preparation of Ni-loaded lignite char catalyst. The MM coal as the untreated coal and the five treated coals from Section 2.2.1 were used as supports for preparing the Ni-loaded lignite char catalyst. The Ni loadings of all catalysts were controlled to provide approximately 20 wt%.[2,14,23] The preparation process of the Ni-loaded lignite char catalyst was divided into two stages.

The first stage was the preparation of Ni-loaded lignite coal. A basic hexa-amine nickel carbonate solution ($(NH_3)_6NiCO_3$) was prepared by the mixing of $NiCO_3 \cdot 2Ni(OH)_2 \cdot 4H_2O$ (Sigma Aldrich), $(NH_4)_2CO_3$ (QReC), NH_4OH (Carlo Erba) and distilled water. The untreated and treated coals were mixed with $(NH_3)_6NiCO_3$ solution for 24 h at room temperature for the ion exchange. The ion-exchanged coals were filtered and washed with DI water until neutral. The modified coals were dried for 24 h at 107 °C and the prepared Ni-loaded lignite coal was completed and collected in a desiccator.

In the second stage of the preparation of the Ni-loaded lignite char catalyst, 1 g of Ni-loaded lignite coals were mixed with 25 g of sand (with a particle size of 1–2 mm) to provide a 2 cm high catalyst bed. The mixture was added into the catalytic reactor and pyrolyzed in a flow of N_2 atmosphere at 120 ml min^{-1} from ambient temperature to 650 °C for 30 min and

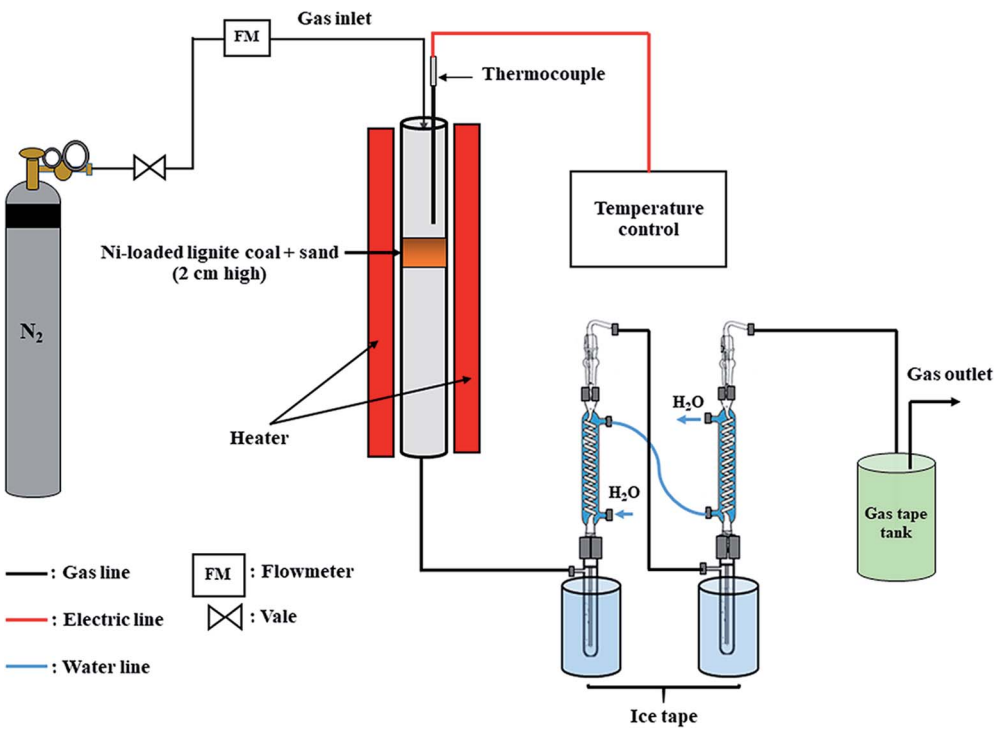

Fig. 2 Schematic diagram of the experimental setup for Ni-loaded lignite char catalyst preparation.

held for 1 h. The schematic diagram of the experimental setup for the Ni-loaded lignite char catalyst preparation is shown in Fig. 2. The catalyst samples were called Ni/MMchar, Ni/HClMMchar, Ni/AceMMchar, Ni/NaMMchar, Ni/NaHClMMchar and Ni/NaAceMMchar according to the preparations in 2.2.1.

2.3 Analytical methods

The functional groups of the Ni-loaded lignite coal samples and Ni-loaded lignite char catalysts were measured by Attenuated Total Reflectance Fourier Transform Infrared Spectroscopy (ATR-FTIR, PerkinElmer, Frontier). The ATR-FTIR spectra were recorded in the scan range of 500–4000 cm^{-1} at a resolution of 4 cm^{-1}.

The Ni contents in the catalysts were analysed by Atomic Absorption Spectroscopy (PerkinElmer, AAnalyst 100) was done according to ASTM D 3683.

The phase and crystallinity of Ni-loaded lignite catalysts were analysed by X-ray diffraction in the powder mode (Phillips X-'pert) using CuK radiation (20 kV, 20 mA) with a scanning speed of 5° min^{-1}. The data were characterized using the Joint Committee on Powder Diffraction Standards (JCPDS).

The surface morphologies of the catalysts were investigated by field emission scanning electron microscopy and energy-dispersive X-ray spectroscopy (FESEM-EDS, JEOL JSM-6335F).

The thermal behaviours and stabilities of the catalysts were determined by TGA-DTG analysis. Firstly, the samples were dried at 105 °C for 60 min. Then, 10 mg of samples were contained in an Al_2O_3 pan for testing in a simultaneous thermal analyser (STA, Rigaku, Thermo plus EVO2). The temperature-programmed pyrolysis was conducted under N_2 flow from ambient temperature to 1000 °C at 10 °C min^{-1}. The results of thermogravimetry (TG) and derivative thermogravimetry (DTG) were obtained using the software of the analyser.

3. Results and discussion

3.1 Raw material

MM coal was represented as a lignite coal sample in this study because it was the main lignite coal in Thailand. The properties of MM coal are summarized in Table 1. The MM coal had a high ash content (14.00 wt%), low total sulphur content (1.01 wt%) and high oxygen content (23.21 wt%).

In Table 2, the properties of the MM coal were compared with the other coals that were used in the preparation of Ni-loaded lignite char catalysts such as Loy Yang coal, Yollourn coal, Eco coal and Shengli coal. MM coal had higher ash content (14.00 wt%) as compared to the other coals, which indicated the high mineral matter. Generally, the mineral matter in coals can be divided into three different types: (i) dissolved salts and other inorganic substances in the coal's pore water, (ii) exchangeable metallic species associated with the organic structure of the coal matrix, and (iii) discrete inorganic particles (crystalline or non-crystalline), representing true mineral components.[8,24] For low-rank coal like lignite, most of the mineral matter is usually exchangeable metallic species such as Na^+, K^+, Ca^{2+} and Mg^{2+}. These exchangeable metallic species are associated with the oxygen-containing functional groups in the form of carboxylate.[8] Possible positions of the exchangeable metallic species in the coal structure are shown in Fig. 3.

Table 3 indicates the major chemical composition of MM coal in weight percentage obtained from XRF analysis in terms of oxide compounds. The large metal elements in MM coal were mainly Ca, Al, Mg, Na and Fe, and the quantities of CaO, Al_2O_3,

Table 2 Coal properties[a]

Coal	Properties (wt%) VM_d	FC_d	A_d	S_t	Ref.
Loy Yang	54.80	44.40	0.70	0.20	2
Yollourn	53.30	45.00	1.60	0.30	3
Eco	53.40	42.70	4.20	0.10	4
Shengli	43.20	50.30	6.50	0.30	5
Mae Moh	41.48	44.52	14.00	1.00	This study

[a] VM: volatile matter, A: ash content, FC: fixed carbon, S_t: total sulphur content, d: dried basis.

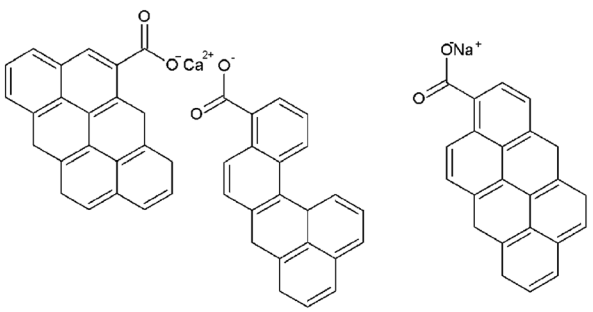

Fig. 3 Possible positions of the exchangeable metallic species in the coal structure.[8]

Table 1 Properties of Mae Moh coal[a]

Proximate analysis (wt%) M_{ar}	VM_d	A_d	FC_d[b]	Ultimate analysis (wt%, daf) C	H	N	O[b]	S_t (wt%)	Calorific value (cal g^{-1})
19.62	41.48	14.00	44.52	69.36	4.80	2.63	23.21	1.01	3804

[a] M: moisture, VM: volatile matter, A: ash content, FC: fixed carbon, S_t: total sulphur, ar: as received basis, b: by difference, d: dried basis and daf: dried and ash-free basis.

MgO, Na_2O and Fe_2O_3 were 20.09, 13.29, 8.64, 6.40 and 5.79 wt%, respectively. Ni in the form of NiO was present in a small amount, 1.19 wt%, in MM coal. Among the main metal elements, Ca and Mg, in particular, might be the exchangeable metallic species. According to Ward,[25] one-half of the calcium and most of the magnesium in Mea Moh coal were found in the form of exchangeable metallic species. As a result, it was possible that the difference in ash content might be correlated to the exchangeable metallic species contained in coal and influenced the Ni ion-exchange mechanism of the preparation of Ni-loaded lignite char catalyst. Consequently, MM coal was quite suitable for use as a catalyst supporter in this study. To prove this assumption, MM coal was treated to remove the ash content. However, the coal treatment involved several methods, namely acid treatment, alkali treatment and alkali followed by acid treatment. Each of the coal treatment methods had different effects on the ash removal and the Ni ion-exchange mechanism. Therefore, these treatments were applied in this research and their results are discussed in the next section.

3.2 Coal treatment

3.2.1 The effect of coal treatment on ash removal. The influences of coal treatment on the Ni ion-exchange mechanism for the preparation of Ni-loaded lignite char catalyst were investigated. Firstly, Mae Moh coal was subjected to different treatments as mentioned in the previous section. The properties of untreated and treated coals are presented in Table 4.

According to the results in Table 4, it was observed that the various treatment processes affected the coal properties, especially the ash content. Compared with MM coal, the ash contents of HClMM and AceMM coals decreased by 80.43% and 55.14%, respectively. In the case of alkali treatment, the ash content of NaMM coal decreased by 6.64%. This indicated that the NaOH solution had a negligible effect on the ash removal of coal. When NaMM coal was treated with HCl and CH_3COOH in the alkali followed by acid treatment, the ash contents of NaHClMM and NaAceMM coals decreased by 72.57 and 27.50%, respectively. The decreases in the ash content could indicate the reduction of the mineral matter content in the modified coals. From the results of coal treatments, the large decrease in the ash content of the MM coal resulted from the coal treatments with acid solutions. Moreover, this research found that the removal of ash from coal depended upon the type of acid solution. The coal treatment with HCl had a greater effect on ash removal than CH_3COOH because HCl is a strong acid that was virtually 100% ionised in solution. Thus, the HCl solution diffused and dissolved mineral matters in coal more than CH_3COOH, a weak acid. Besides, the difference in ash removal by the various acids could be explained by the ability of the acids to remove different inorganic components. According to the study by Barma *et al.*,[26] HCl could dissolve impurities in coal by converting them into soluble metal salts. Steel *et al.*[27] reported that HCl was able to remove Ca, Fe, Mg, Na and some of Al, K and Ti, which were minerals in coal. Manoj *et al.*[28] discovered that acetic acid solution could remove all calcites and partial aluminium minerals in coal and transform them into calcium acetate and aluminium acetate complexes. Therefore, the changes in the ash content in MM coal are related to the mineral matter in coal, especially exchangeable metallic species that might affect the changes in the functional groups in coal. The results of the influences of coal treatments on the functional groups in coal were studied and are discussed in the following section.

Table 4 Properties of untreated and treated coals[a]

Coal sample	Properties (wt%)				Ash removal (%)
	VM_d	A_d	FC_d	S_t	
MM coal	41.48	14.00	44.53	1.01	—
HClMM coal	42.29	2.75	54.95	1.04	80.43
AceMM coal	41.93	6.29	51.78	1.04	55.14
NaMM coal	37.96	13.07	48.98	1.01	6.64
NaHClMM coal	42.36	3.84	53.82	1.10	72.57
NaAceMM coal	40.34	10.14	49.51	1.10	27.50

[a] VM: volatile matter, A: ash content, FC: fixed carbon, S_t: total sulphur content, d: dried basis.

3.2.2 The effect of coal treatment on functional groups. As previously described, the treatments affected the ash content in coal. They resulted in the removal of exchangeable metallic species, which make up most of the mineral matter in low-rank coal. These metallic species are associated with the oxygen-containing functional groups that are presented in the form of metal-carboxylate. Therefore, eliminating exchangeable metallic species from coal might affect the metal-carboxylate in coal, impacting the functional groups in coal. To investigate the influence of treatments on the functional groups in coal, the FTIR spectra of untreated and treated coals are presented in Fig. 4. The assignments of the IR bands in the FTIR spectra of untreated and treated coals are summarized in Table 5.

In Fig. 4a, the FTIR spectrum shows IR bands of the major functional group characteristics of the MM coal compositions. The IR band at 3408 cm^{-1} was assigned to phenolic hydroxyl associated hydrogen bonds. The double IR bands at 2921 and 2851 cm^{-1} were attributed to cycloalkane or methylene of aliphatic hydrocarbons.[29] The IR bands at 1560 and 1455 cm^{-1} were assigned to the aromatic structure.[31] The two bands of the metal-carboxylate groups were observed at 1560 and

Table 3 The main chemical composition of MM coal (wt%) by XRF

	Fe_2O_3	Al_2O_3	MgO	SiO_2	CaO	K_2O	Na_2O	TiO_2	MnO_2	P_2O_5	SO_3	NiO
MM coal	5.79	13.29	8.64	23.92	20.09	1.34	6.40	0.25	0.14	0.42	18.53	1.19

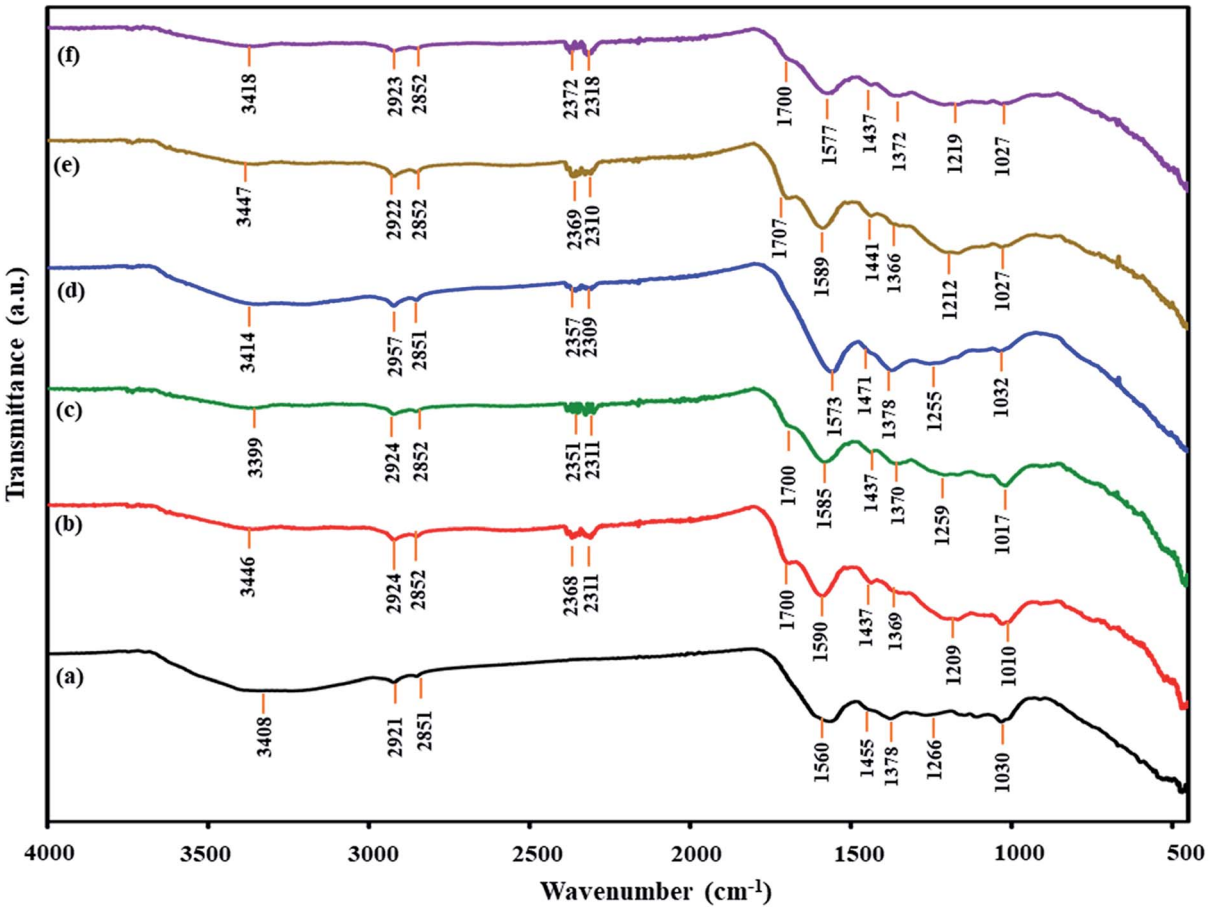

Fig. 4 FTIR spectra of untreated and treated coals: (a) MM coal, (b) HClMM coal, (c) AceMM coal, (d) NaMM coal, (e) NaHClMM coal and (f) NaAceMM coal.

Table 5 FTIR assignment of untreated and treated coal[a]

	Wavenumber, ϑ (cm^{-1})						
Assignments of band	MM	HClMM	AceMM	NaMM	NaHClMM	NaAceMM	Ref.
–OH stretching vibration of hydrogen bond association, phenols	3408	3446	3399	3377	3414	3418	29
Non-symmetric vibration of cycloalkane or methylene of aliphatic hydrocarbons	2921	2924	2924	2923	2922	2923	29
Symmetric vibration cycloalkane or methylene of aliphatic hydrocarbons	2851	2852	2852	2851	2852	2852	29
–OH stretching vibration of –COOH	ND	2368	2357	2357	2364	2318	30
C=O stretching of carboxyl groups	ND	1707	1700	ND	1707	1700	29
C=O asymmetric stretching of carboxylate ($\vartheta_{as}(CO_2^-)$)	1560	1590	1585	1573	1589	1577	31
Stretching vibration of aromatic C–C	1455	1437	1437	1471	1441	1437	31
C=O symmetric stretching of carboxylate ($\vartheta_s(CO_2^-)$)	1378	1369	1370	1378	1366	1372	31
C–O stretching	1031	1027	1017	1012	1027	1027	31

[a] ND: not detected.

1378 cm^{-1}.[31] The IR band at 1030 cm^{-1} was ascribed to the C–O stretching.[29]

For the acid treatment, the FTIR spectra of HClMM and AceMM coals are presented in Fig. 4b and c, respectively. The IR band of HClMM coal appeared in new bands at 2368, 2311 and 1700 cm^{-1}. Likewise, the new bands of AceMM coal were observed at 2351, 2311 and 1700 cm^{-1}. The IR bands at 2780–2350 cm^{-1} could be assigned to the –OH stretching vibration of

–COOH.[30] The IR band at 1700 cm^{-1} could be attributed to the C=O of carboxyl groups.[31] The appearances of new bands on the IR spectra of both acid-treated coals indicated that carboxyl groups were formed in both the acid-treated coals. Moreover, the two bands of metal-carboxylate groups were observed at 1610–1550 cm^{-1} ($\vartheta_{as}(CO_2^-)$) and 1420–1300 cm^{-1} ($\vartheta_s(CO_2^-)$) in the FTIR spectra of HClMM and AceMM coals. From the literature reviews,[32,33] the separation of the two bands of metal-carboxylate groups ($\Delta\vartheta(COO^-) = \vartheta_{as}(CO_2^-) - \vartheta_s(CO_2^-)$) were indicative of the structure of a given carboxylate. According to Ban *et al.*,[34] the addition of metal ions on coal caused the decrease in the $\Delta\vartheta(COO^-)$ value due to metal-carboxylate interactions. It was assumed that the metal ions were combined with carboxyl functional groups in coal by ionic configuration. Conversely, this research found that the $\Delta\vartheta(COO^-)$ values increased when the MM coal was treated with HCl or CH_3COOH solutions. In Table 6, the $\Delta\vartheta(COO^-)$ values of HClMM and AceMM coals increased from 188 cm^{-1} to 221 cm^{-1} and 215 cm^{-1}, respectively. Therefore, the increase in $\Delta\vartheta(COO^-)$ of HClMM and AceMM coals might indicate that the metal ions that interacted with carboxyl functional groups in the form of metal-carboxylate were removed from the coal. From the results, the appearances of new bands of carboxyl groups and the increase in the $\Delta\vartheta(COO^-)$ values of both acid-treated coals could explain that the acid solution ionised to give protons (H^+). Then, the protons of the acid were exchanged with the metal ions of metal-carboxylate (COOM) in coal (eqn (2)). Due to the ion exchange of protons and metal ions, the carboxyl groups were formed in coal. After that, the released metal ions (M^+) were exchanged with Cl^- for HCl (eqn (3)) and CH_3COO^- for CH_3COOH (eqn (4)) in the form of acid-soluble salts, which resulted in ash removal in coal.

$$COOM + H^+ \rightarrow COOH + M^+ \quad (2)$$

$$M^+ + Cl^- \rightarrow MCl \quad (3)$$

$$M^+ + CH_3COO^- \rightarrow CH_3COOM \quad (4)$$

In the case of alkali treatment, Fig. 4d shows the FTIR spectrum of NaMM coal. Compared with original coal, the FTIR ranges of NaMM coal changed a little. The new bands of the –OH stretching vibrations of –COOH were observed at 2357 and 2309 cm^{-1}. These occurrences of the new bands might be due to the alkali solution, which could donate hydroxide ions to coal.[35] In Table 6, the (COO^-) values of NaMM coal slightly increased from 188 cm^{-1} to 195 cm^{-1}, which indicated that NaOH treatment could hardly remove the metal ions from metal-carboxylate in coal.

For alkali followed by acid treatment, the NaMM coal was treated with HCl and CH_3COOH solutions. The FTIR spectrum of NaHClMM coal (Fig. 4e) showed new IR bands at 2369, 2310 and 1707 cm^{-1}. The FTIR spectrum of NaAceMM coal (Fig. 4f) presented the new bands at 2372, 2318 and 1700 cm^{-1}. The appearances of new IR bands of NaHClMM and NaAceMM coals indicated the occurrence of carboxyl groups in coals. In Table 6, the $\Delta\vartheta(COO^-)$ values of NaHClMM coal and NaAceMM coal increased higher than the NaMM coal. The $\Delta\vartheta(COO^-)$ values of NaMM and NaHClMM and NaAceMM coals were 195 cm^{-1}, 221 cm^{-1} and 205 cm^{-1}, respectively. It was indicated that after the NaMM coal was treated with acid solutions, the metal ions of metal-carboxylate groups were removed and were replaced with hydrogen ions from acid solutions. In conclusion, the changing functional groups of NaHClMM and NaAceMM coals were mainly caused by the acid treatments.

3.3 Ni loading on lignite coal

As described earlier, the coal treatments with acid or alkali solutions influenced the functional groups in coal, especially the oxygen-containing functional groups such as hydroxyl and carboxyl groups. These oxygen-containing groups in low-rank coal were cation-exchange sites for exchanging with metal ions on the coal surface. It was noted that treated coals had differences in ash content and functional groups. Thus, the coal treatments might affect the coal properties, including functional groups that might impact the Ni loading mechanisms into coals. To investigate the influence of coal treatments on the Ni loading mechanisms, FTIR spectra of untreated and treated coals before and after Ni loading were studied.

3.3.1 Untreated coal. The FTIR spectra of MM coal before and after Ni loading are presented in Fig. 5. When Ni ions were loaded on the MM coal, the peak intensity of hydroxyl at around 3368 cm^{-1} of MM coal decreased. The IR bands at 2200–1955 cm^{-1} were observed on the FTIR pattern of MM coal after

Table 6 Carboxylate asymmetric ($\vartheta_{as}(CO_2^-)$) and symmetric ($\vartheta_s(CO_2^-)$) vibrational frequencies for the $\Delta\vartheta(COO^-)$ values of untreated and treated coals

	Untreated and treated coals (before Ni loading)			Untreated and treated coals (after Ni loading)		
Coal sample	$\vartheta_{as}(CO_2^-)$ (cm^{-1})	$\vartheta_s(CO_2^-)$ (cm^{-1})	$\Delta\vartheta(COO^-)$ (cm^{-1})	$\vartheta_{as}(CO_2^-)$ (cm^{-1})	$\vartheta_s(CO_2^-)$ (cm^{-1})	$\Delta\vartheta(COO^-)$ (cm^{-1})
MM	1560	1372	188	1548	1375	173
HClMM	1590	1369	221	1558	1375	183
AceMM	1585	1370	215	1566	1375	191
NaMM	1573	1378	195	1547	1376	171
NaHClMM	1589	1366	221	1558	1375	183
NaAceMM	1577	1372	205	1559	1379	180

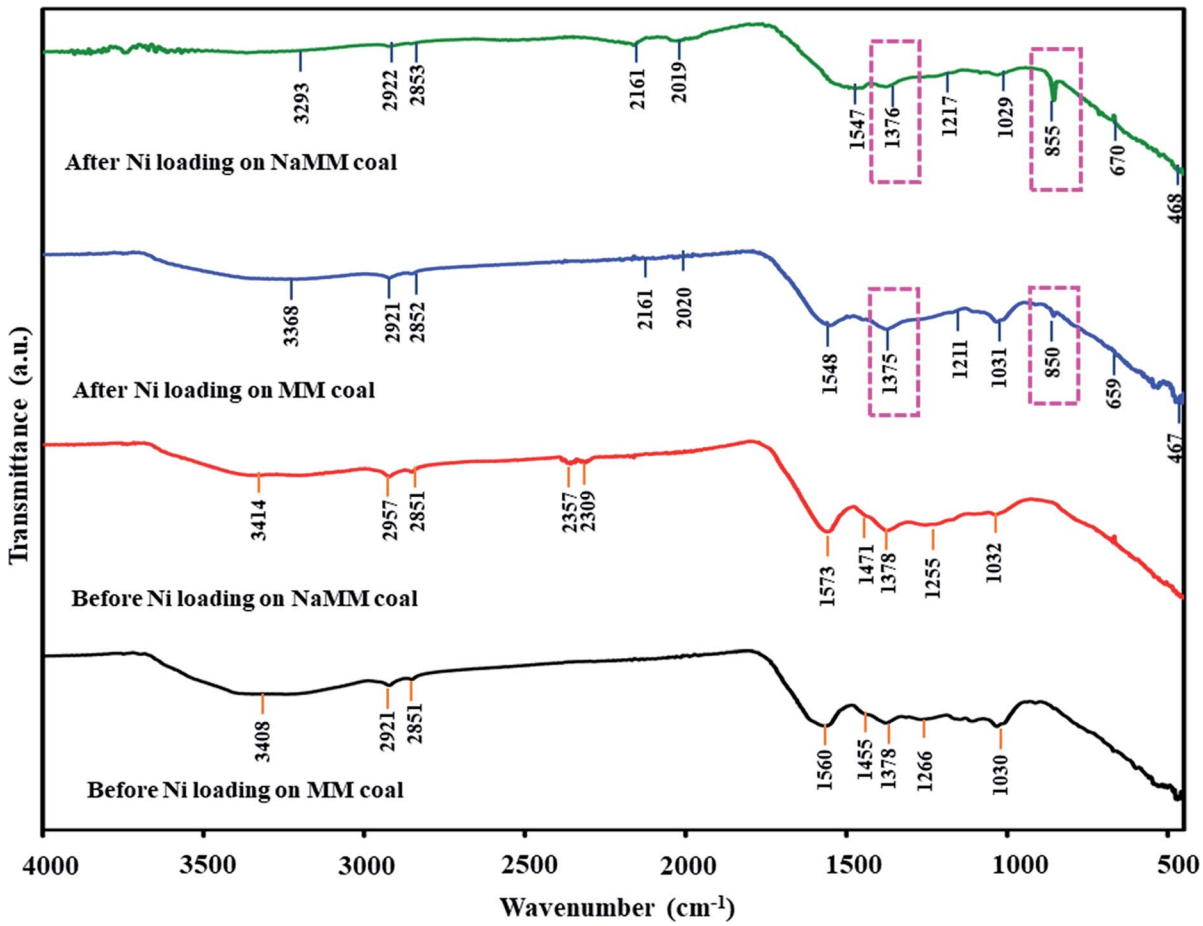

Fig. 5 FTIR spectra of MM coal and NaMM coal before and after Ni loading.

Ni loading, which was assigned to transition metal carbonyl complexes. The band appearances of the transition metal carbonyl complexes in the FTIR pattern were in accord with a study by Sarkar *et al.*[36] In Table 6, the $\Delta\vartheta(COO^-)$ after Ni loading on MM coal decreased from 188 to 173 cm^{-1} when compared with before Ni loading. This indicated that Ni ions were exchanged with the released H^+ ions from hydroxyl groups and converted into the metal-carboxylate. Besides, the IR bands within the range of 1350–1550 cm^{-1} were observed in the FTIR spectrum of MM coal after Ni loading, which revealed carbonate phases. The occurrence of carbonate phases after Ni loading was confirmed by the band at 850 cm^{-1}. The appearances of two bands of carbonate phases in the FTIR spectra corresponded to results obtained by Kledyński *et al.*[37] From the results mentioned above, it is likely that Ni ions were exchanged with metal ions (M^+) of metal-carboxylate groups on coal. After that, the released metal ions (M^+) from metal-carboxylate groups were exchanged with carbonate ions (CO_3^{2-}) from the $(NH_3)_6$-$NiCO_3$ solution into carbonate salts during the ion-exchange method.

Considering the form of Ni ion that was exchanged with the functional groups on MM coal, it was found that Ni ions might be exchanged with the functional groups on MM coal in the form of the $Ni(NH_3)_6^{2+}$ ion. This was because the FTIR spectrum of MM coal after Ni loading showed the IR bands of $Ni(NH_3)_6^{2+}$ that consisted of $\nu(NH_3)$, $\delta_s(HNH)$, $\rho_r(NH_3)$ and $\nu(M-NH_3)$ in the regions of 3386–3156, 1254–1186, 850–650 and 500–250 cm^{-1}, respectively.[38,39] In Fig. 6, the FTIR spectra of MM coal after Ni loading showed the IR bands of $Ni(NH_3)_6^{2+}$ at 3368, 1211, 659 and 467 cm^{-1}. Moreover, the form of Ni ion after Ni loading on coal could be observed from the pH of the $(NH_3)_6$-$NiCO_3$ solution after the ion-exchange process. From the literature reviews,[40,41] Sharma *et al.*[40] studied the ion exchange of Ni on a meta-acrylic acid type ion exchange resin as the carbon base, and Cao *et al.*[41] loaded Ni on resin char *via* the ion-exchange method. Both of these reports indicated that the pH of the aqueous ammonia solution used in the ion exchange affected the form of the Ni ion on the resin. The Ni ion was exchanged as the $Ni(H_2O)_6^{2+}$ ion at pH 8.8, and as the $Ni(NH_3)_6^{+2}$ ion at pH 9.4.[40] Likewise, the pH value of the $(NH_3)_6NiCO_3$ solution after Ni loading on MM coal in this study was 9.5 as shown in Table 7. It confirmed that Ni ions in the form of $Ni(NH_3)_6^{2+}$ ions were exchanged with MM coal. Thus, the mechanism of Ni loading on MM coal can be shown as eqn (5)–(7).

$$-OH + Ni(NH_3)_6^{2+} \leftrightarrow O[Ni(NH_3)_6] + H^+ \quad (5)$$

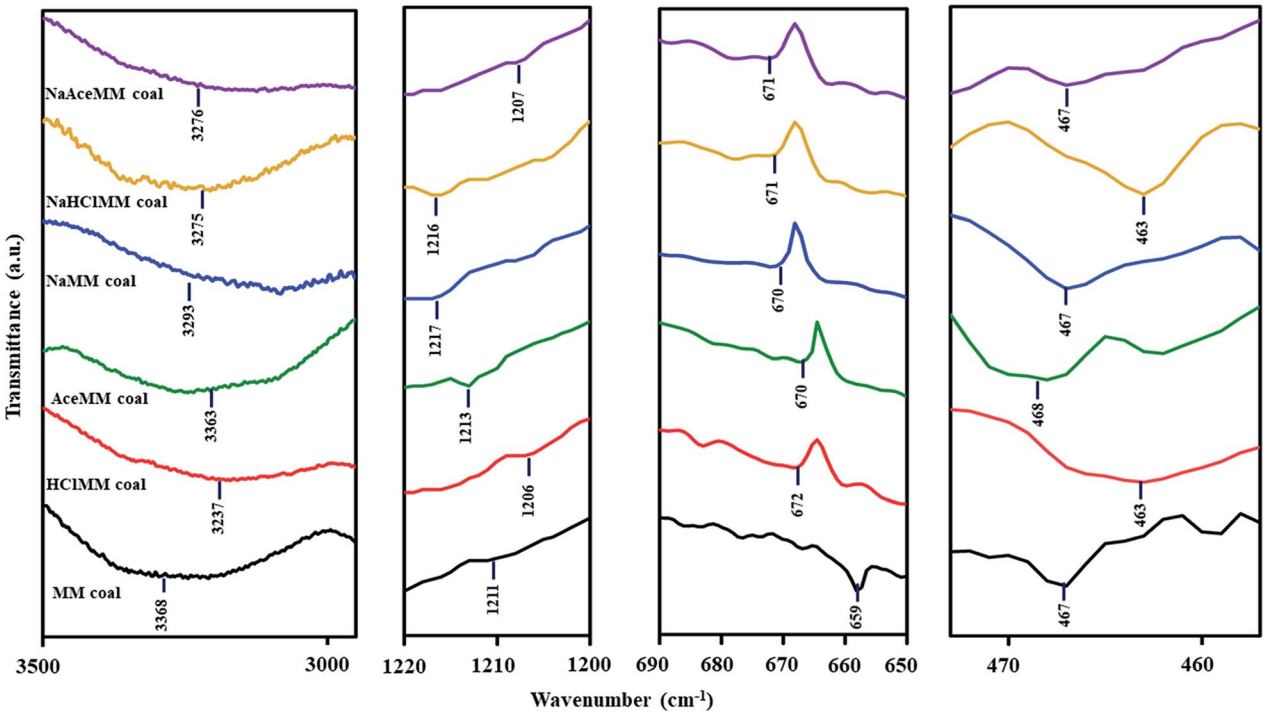

Fig. 6 FTIR spectra of $Ni(NH_3)_6^{2+}$ untreated coal and treated coal after Ni loading.

Table 7 pH values of $(NH_3)_6NiCO_3$ solutions after the Ni loading of untreated and treated coals

Coal	MM	HClMM	AceMM	NaMM	NaHClMM	NaAceMM
pH of solution	9.5	8.4	9.0	9.6	9.6	9.6

$$2COOM^+ + Ni(NH_3)_6^{2+} \leftrightarrow COO[Ni(NH_3)_6]OOC + 2M^+ \quad (6)$$

$$M^+ + CO_3^{2-} \leftrightarrow M_2CO_3 \quad (7)$$

In comparison with the ion exchange of metal ions on the other lignite (*e.g.*, Yallourn coal and Adaro coal),[42,43] it was found that the ion exchange of metal ions on most lignite coals occurred through hydroxyl and carboxyl groups on the coal. This was because the structure of these lignite coals was composed of hydroxyl and carboxyl groups. This contrasted with MM coal, in which carboxyl groups disappeared in the structure of coal, but the FTIR bands of MM coal indicated hydroxyl and metal-carboxylate groups. The metal-carboxylate in the structure of MM coal might result from the abundance of exchangeable metallic species such as Ca, Na and Mg in MM coal, as presented in Table 3. Some researchers reported that the exchangeable metallic species in low-rank coal were usually found in the form of metal-carboxylate groups.[8,25] Therefore, the ion exchange of Ni ion in MM coal occurred through hydroxyl and metal-carboxylate groups.

3.3.2 Acid treatment. The coal sample was treated with different acid solutions, namely HCl and CH_3COOH solutions. As indicated in Section 3.2, the coal treatments with both acid solutions were able to reduce the ash content in coal and changed the functional group on MM coal, especially the conversion of metal-carboxylate groups into carboxyl groups. Due to acid treatment, the changes in the functional groups might affect the mechanism of Ni loading on MM coal. Both acid-treated coals were loaded with Ni by the ion-exchange method; the FTIR results of HClMM and AceMM coals before and after Ni loading are presented in Fig. 7. The results showed that the IR bands of the –OH stretching vibration of –COOH at 2780–2350 cm^{-1}, and the band intensity of C=O of carboxyl groups at 1700 cm^{-1} decreased in the FTIR patterns of HClMM and AceMM coals after Ni loading. Meanwhile, the new IR bands of transition metal carbonyl complexes at 2200–955 cm^{-1} were observed in the FTIR patterns of both acid-treated coals after Ni loading. In Table 6, the $\Delta\vartheta(COO^-)$ values of HClMM and AceMM coals after Ni loading also decreased in comparison with HClMM and AceMM coals before Ni loading. From the FTIR results of acid-treated coals in the case of after Ni loading, the decrease in the band intensity of carboxyl groups indicated that the carboxyl groups on coal were exchanged with Ni ions and turned into metal-carboxylates. The interaction of the metal-carboxylate on acid-treated coals could also be confirmed by the decrease in $\Delta\vartheta(COO^-)$ values. The reductions in the

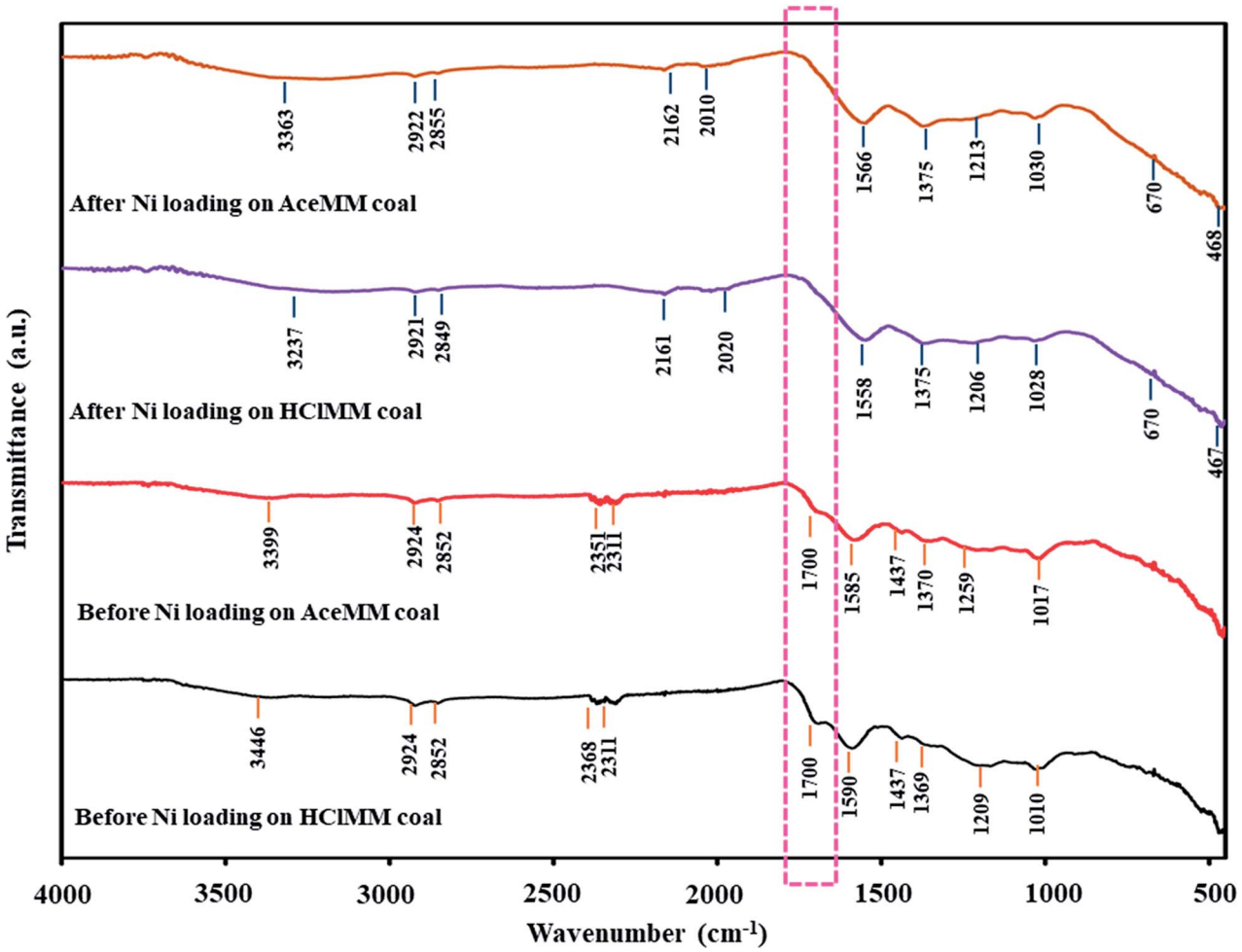

Fig. 7 FTIR spectra of acid-treated coals before and after Ni loading.

carboxyl band intensities on acid-treated coals after Ni ion exchange in this study also corresponded to the metal loading on the acid-treated coal in the other literature. Li *et al.*[44] indicated that the ion exchange of Na^+ on the acid-treated coal resulted in a decrease in the band intensity of carboxyl groups. Moreover, Ban *et al.*[31] reported that the addition of Ca^{2+} and K^+ on acid-treated coal led to the decrease in the band intensity of the C=O absorption peak at 1700 cm^{-1}. This implied that the carboxyl groups were converted into metal-carboxylates.

On comparing the Ni loading mechanisms of the acid-treated coals and the untreated coal, it was observed that the Ni ions that were exchanged with the carboxyl groups in both acid-treated coals differed from those of the untreated coal. The ion exchange of Ni ions on untreated coal occurred through hydroxyl and metal-carboxylate groups. This was because the coal treatment with HCl and CH_3COOH could decrease the ash content in MM coal from 14.00 wt% to 2.75 wt% and 6.25 wt%, respectively, as shown in Table 4. The decreased ash content in acid-treated coals correlated with the reduction of the exchangeable metallic species content in the metal-carboxylate form, which resulted in the conversion of metal-carboxylate groups into carboxyl groups. As a result, the ion exchange of Ni ions was controlled through the carboxyl groups on acid-treated coals. This could mean that the content of exchangeable metallic species in coal affected the ion exchange of the Ni ions in the coal. In the case of low exchangeable metallic species content in HClMM coal and AceMM coal, the ion exchange of Ni ions could occur through the carboxyl groups in the coal. In contrast, for the ion exchange of Ni ions in the MM coal, which had a high content of exchangeable metallic species, the Ni ions could exchange with the metal-carboxylate groups.

Focusing on the form of Ni ions on acid-treated coals after Ni loading, the –OH stretching vibration in the region of 3600–3200 cm^{-1} and the –OH bending vibration at around 1640 cm^{-1} (ref. 45 and 46) were observed in the FTIR spectrum of HClMM coal after Ni loading. The appearances of both bands on HClMM coal after Ni loading could be assigned to H_2O, which arose from the ion exchange with Ni in the form of $Ni(H_2O)_6^{2+}$ ions on HClMM coal. According to the description of the FTIR spectrum of $[Ni(H_2O)_6](NO_3)_2$ by Liang *et al.*,[47] the broad band of the –OH stretching vibration mode was at around 3400 cm^{-1} and the band of the –OH bending vibration mode was 1640 cm^{-1} on the FTIR spectrum of $[Ni(H_2O)_6](NO_3)_2$. The two bands could be attributed to H_2O. The appearances of H_2O

bands in $[Ni(H_2O)_6](NO_3)_2$ referred to H_2O, which were the composition of the $Ni(H_2O)_6^{2+}$ ion. Moreover, the ion exchange of Ni in the form of $Ni(H_2O)_6^{2+}$ ions on HClMM coal could also be confirmed by the pH values of $(NH_3)_6NiCO_3$ solutions after Ni loading, which was 8.4 as seen in Table 7. Meanwhile, the IR bands of $Ni(NH_3)_6^{2+}$ were also observed at 3237, 1206, 672 and 463 cm^{-1} on the FTIR pattern of HClMM coal after Ni loading, as shown in Fig. 6. The appearances of $Ni(NH_3)_6^{2+}$ bands on HClMM coal indicated that Ni ions could be exchanged with HClMM coal in the form of $Ni(NH_3)_6^{2+}$ ions. Therefore, Ni ions were able to exchange with the functional groups on HClMM coal in the forms of $Ni(H_2O)_6^{2+}$ and $Ni(NH_3)_6^{2+}$ ions. The examples of the mechanisms of Ni loading on HClMM are presented as eqn (8) and (9), respectively.

$$2COOH + Ni(H_2O)_6^{2+} \leftrightarrow COO[Ni(H_2O)_6]OOC + 2H^+ \quad (8)$$

$$2COOH + Ni(NH_3)_6^{2+} \leftrightarrow COO[Ni(NH_3)_6^{2+}]\,OOC + 2H^+ \quad (9)$$

For AceMM coal, the FTIR spectrum after Ni loading showed the IR bands of $Ni(NH_3)_6^{2+}$ at 3363, 1213, 670 and 468 cm^{-1}, as seen in Fig. 6. Besides, the pH of $(NH_3)_6NiCO_3$ solutions after the Ni loading of AceMM coal was 9.0, as shown in Table 7. Hence, the functional groups such as carboxyl groups on AceMM coal were in conjunction with Ni ions in the form of $Ni(NH_3)_6^{2+}$ ions according to eqn (9).

3.3.3 Alkali treatment. The FTIR results of alkali-treated coals after Ni loading are presented in Fig. 5. The peak intensities of hydroxyl groups at around 3293 cm^{-1} decreased after Ni loading. The IR bands of transition metal carbonyl complexes were observed at 2161 and 2019 cm^{-1} in the FTIR spectrum of NaMM coal after Ni loading, which indicated that Ni ions were exchanged with hydroxyl groups on NaMM coal. Besides, the two bands of carbonate phases at 1375 cm^{-1} and 855 cm^{-1} appeared in the FTIR spectrum of NaMM coal after Ni loading. The IR band of the carbonate phase at 855 cm^{-1} for NaMM coal after Ni loading showed a high peak intensity. This was probably because of the increase in Na ions on NaMM coal, which remained after NaOH treatment. These residual Na ions might be exchanged with carbonate ions and transformed into Na_2CO_3, which resulted in the high peak intensity of the carbonate phases at 855 cm^{-1}. The formation of Na_2CO_3 on alkali-treated coal was confirmed *via* XRD analysis, as presented in Fig. 9 (Section 3.4). Considering the form of Ni ions in NaMMcoal after Ni loading, it was found that Ni ions were exchanged with functional groups on NaMM coal in the form of

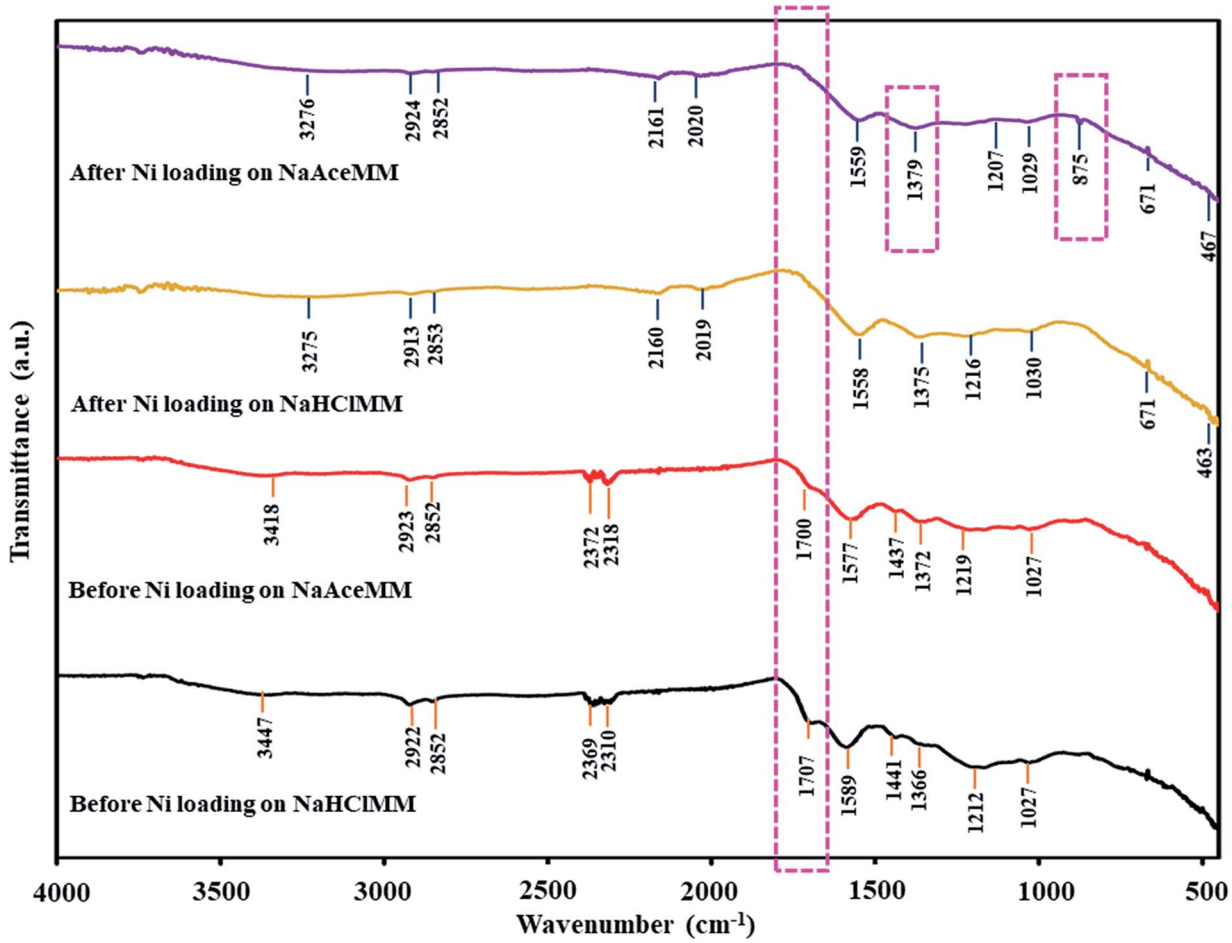

Fig. 8 FTIR spectra of alkali followed by acid treatment of coal before and after Ni loading.

$Ni(NH_3)_6^{2+}$ ions. As shown in Fig. 6, the IR bands of the $Ni(NH_3)_6^{2+}$ ions at 3293, 1213, 670 and 468 cm^{-1} were observed on the FTIR spectrum of NaMM coal after Ni loading. Moreover, the pH value of the $(NH_3)_6NiCO_3$ solution after Ni loading on NaMM was also 9.6, as presented in Table 7. In the case of NaMM coal, the Ni ions were exchanged with hydroxyl and metal-carboxylate groups on NaMM coal, which was similar to the Ni loading behaviour on MM coal as explained in Section 3.3.1.

When the mechanism of the Ni ion exchange on NaMM coal was compared with that of untreated coal, it was observed that the mechanism of the Ni ion exchange on the NaMM coal was similar to the mechanism of the Ni ion exchange on MM coal. This was because the NaOH treatment could slightly remove the ash content in MM coal, which was 6.64% as presented in Table 4. As discussed in Section 3.2.2, the FTIR spectrum of NaMM coal after Ni loading (Fig. 4d) did not have the strong new bands such as carboxyl groups when compared with acid-treated coals (Fig. 4b and c). Hence, the ion exchange of Ni ions on NaMM coal still occurred through the hydroxyl and metal-carboxylate groups that were the same as MM coal. The $\Delta\vartheta(COO^-)$ values of MM coal and NaMM coal after Ni loading were 173 cm^{-1} and 171 cm^{-1}, respectively, which are shown in Table 6. There was a negligible difference in the $\Delta\vartheta(COO^-)$ values of coal.

3.3.4 Alkali followed by acid treatment. FTIR patterns of Ni loading on NaHClMM and NaAceMM coals are shown in Fig. 8. The peak intensities of hydroxyl groups at 3377 cm^{-1} for NaHClMM coal and 3333 cm^{-1} for NaAceMM coal decreased after Ni loading. The IR bands of the –OH stretching vibration of –COOH at 2780–2350 cm^{-1} were not observed on FTIR patterns of NaHClMM and NaAceMM coals after Ni loading. It was also found that the IR bands of C=O of carboxyl groups at 1700 cm^{-1} disappeared on the FTIR patterns of both treated coals after Ni loading. The IR bands of transition metal carbonyl complexes at 2200–955 cm^{-1} were observed in the FTIR patterns of NaHClMM and NaAceMM coals after Ni loading. In Table 6, the $\Delta\vartheta(COO^-)$ values of NaHClMM and NaAceMM coals after Ni loading decreased when compared with before Ni loading. From the FTIR results of NaHClMM and NaAceMM coals, it meant that Ni ions were exchanged with hydroxyl and carboxyl groups in the metal-carboxylate groups. Hydroxyl groups on NaHClMM and NaAceMM coals might have resulted from alkali treatment, while carboxyl groups on both treated coals might be due to acid treatment. In the case of NaAceMM, the two bands of the carbonate phases at 1379 cm^{-1} and 875 cm^{-1} were observed in the FTIR spectrum of NaAceMM coal after Ni loading, indicating that Ni ions were exchanged with metal ions of metal-carboxylate groups on NaAceMM coal. Concentrating on the form of the Ni ions on NaHClMM and NaAceMM coals after Ni loading, the

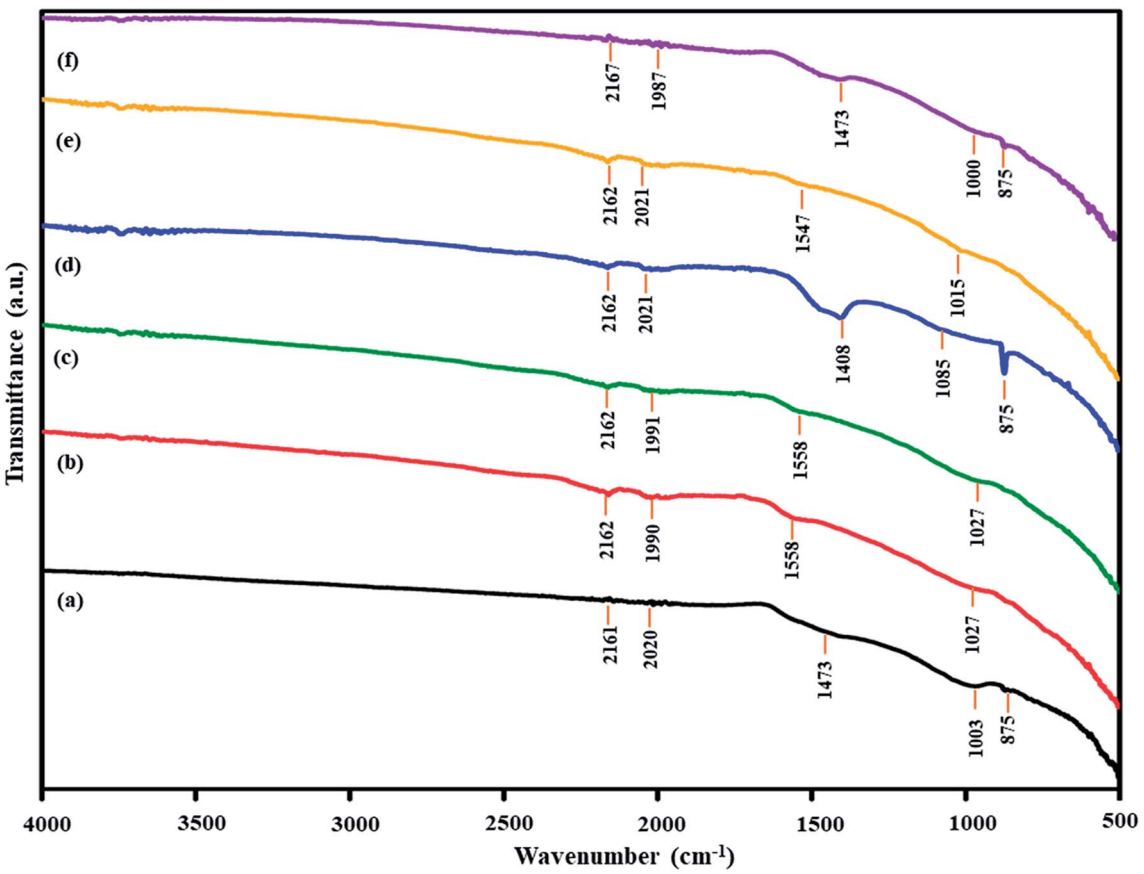

Fig. 9 FTIR spectra of Ni-loaded lignite char catalysts: (a) Ni/MMchar, (b) Ni/HClMMchar, (c) Ni/AceMMchar, (d) Ni/NaMMchar, (e) Ni/NaHClMMchar and (f) Ni/NaAceMMchar.

FTIR of $Ni(NH_3)_6^{2+}$ at 3275, 1216, 671 and 463 cm^{-1} were observed on NaHClMM coal after Ni loading as presented in Fig. 6. Similarly, the FTIR spectrum of NaAceMM coal after Ni loading showed the bands of $Ni(NH_3)_6^{2+}$ at 3376, 1207, 671 and 467 cm^{-1}. The pH values of $(NH_3)_6NiCO_3$ solutions after the Ni loading of both coal samples were 9.6 as shown in Table 7. Thus, the Ni ions were exchanged with functional groups on both types of treated coals in the form of $Ni(NH_3)_6^{2+}$ ions.

As mentioned above, the mechanism of Ni loading on NaHClMM and NaAceMM coals resulted in the exchange of Ni ions with hydroxyl groups and carboxyl groups on both coal samples and converted them into metal-carboxylate groups. In the case of NaAceMM coal, Ni ions were still exchanged with metal-carboxylate groups due to the high ash content of the NaAceMM coal. For the formation of Ni ions on coal after Ni loading, Ni ions were exchanged with the functional groups on both NaHClMM and NaAceMM coals in the form of $Ni(NH_3)_6^{2+}$ ion.

In comparing the mechanisms of the Ni ion exchange of NaHClMM and NaAceMM coals with those of HClMM and AceMM coals, it was found that Ni ions were exchanged with carboxyl groups on NaHClMM and NaAceMM coals, which were the same as with the acid-treated coals. This resulted from the acid treatment leading to the reduction of the ash content in the coal and the conversion of the metal-carboxylate group into the carboxyl group. As a result, the carboxyl groups on both treated coals acted as the Ni ion exchange sites on coals. Additionally, the results of the ion exchange of Ni ions on NaAceMM were found to show that Ni could exchange with metal-carboxylate groups on NaAceMM coal, similar to both MM coal and NaMM coal. Since the percentage of ash removal of NaAceMM coal was 27.50%, it indicated that mineral matter in the form of the metal-carboxylate groups might remain in NaAceMM coal. These metal-carboxylate groups still served as the positions for the ion exchange of Ni on NaAceMM coal.

3.4 Production of Ni-loaded lignite char catalyst

After the Ni loading on coal, Ni-loaded lignite coal samples were pyrolyzed at 650 °C under a N_2 atmosphere to produce Ni-loaded lignite char catalysts. FTIR analysis results of catalysts are shown in Fig. 9. The IR bands of Ni-loaded lignite char catalysts mainly appeared in the range of 2200–1955 cm^{-1}, 1500–1400 cm^{-1} and 1300–1000 cm^{-1}. The IR bands at 2200–1955 cm^{-1} were assigned to transition metal carbonyl complexes. The IR bands at 1500–1400 cm^{-1} correspond to aromatic C–C stretching (in-ring).[48] The IR bands at 1300–1000 cm^{-1} were assigned to C–O stretching vibrations. Moreover, the bands of carbonate phases at 1350–1550 cm^{-1} and 880–860 cm^{-1} were also observed in the FTIR spectra of Ni/MMchar (Fig. 9a), Ni/NaMMchar (Fig. 9d) and Ni/NaAceMMchar (Fig. 9f) catalysts, but not Ni/HClMMchar (Fig. 9b), NiAceMMchar (Fig. 9c) and Ni/NaHClMMchar (Fig. 9e) catalysts. The formation of carbonate phases in the catalysts was also correlated with the XRD analysis results of catalysts. Fig. 10 presents XRD patterns of the Ni-loaded lignite char catalysts at 10–40° for 2θ to show the XRD pattern of the carbonate phases. According to the JCPDS database, the peaks

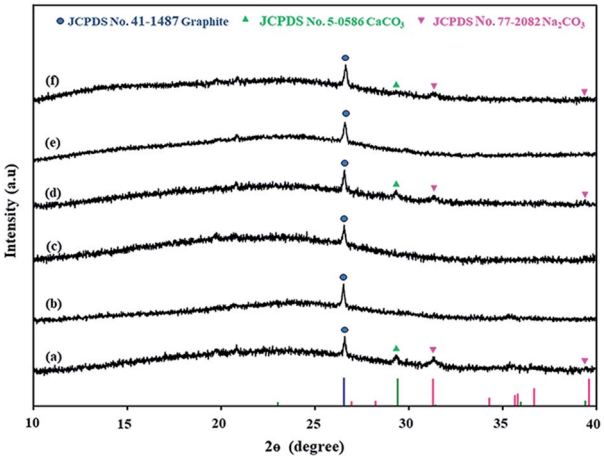

Fig. 10 XRD patterns of Ni-loaded lignite char catalysts at 2θ of 10–40°: (a) Ni/MMchar, (b) Ni/HClMMchar, (c) Ni/AceMMchar, (d) Ni/NaMMchar, (e) Ni/NaHClMMchar and (f) Ni/NaAceMMchar.

corresponding to $CaCO_3$ (JCPDS no. 5-0586) and Na_2CO_3 (JCPDS no. 77-2082) were observed in the XRD patterns of Ni/MMchar (Fig. 10a), Ni/NaMMchar (Fig. 10d) and Ni/NaAceMMchar (Fig. 10f) catalysts. However, the patterns of carbonate compounds were not found in Ni/HClMMchar (Fig. 10b), Ni/AceMMchar (Fig. 10c) and Ni/NaHClMMchar (Fig. 10e) catalysts. The FTIR and XRD results of Ni/MMchar, Ni/NaMMchar and NiNaAceMMchar supported the explanation given in Section 3.3 that Ni ions were able to exchange with the metal ions of metal-carboxylate groups in MM, NaMM and NaAceMM coals. After the ion exchange, the released metal ions were exchanged with carbonate ions from $(NH_3)_6NiCO_3$ and converted into carbonate compounds that remained in the catalyst powder. Regarding the XRD patterns of Ni-loaded lignite char catalysts at 2θ of 10–80° as shown in Fig. 11, Ni was present in the form of metal in the catalysts. This was confirmed by the

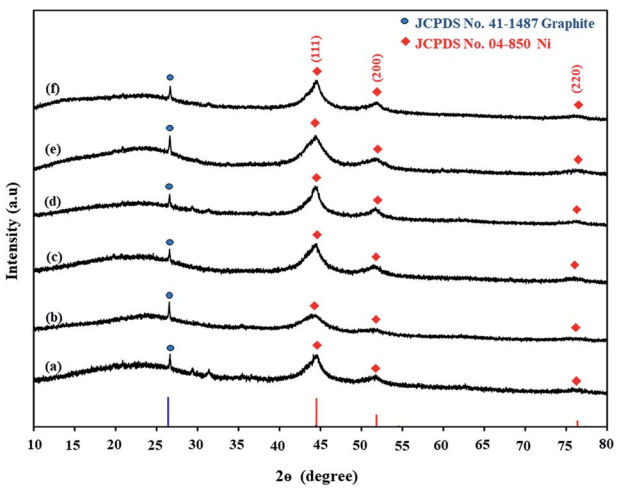

Fig. 11 XRD patterns of Ni-loaded lignite char catalysts at 2θ of 10–80°: (a) Ni/MMchar, (b) Ni/HClMMchar, (c) Ni/AceMMchar, (d) Ni/NaMMchar, (e) Ni/NaHClMMchar and (f) Ni/NaAceMMchar.

three characteristic peaks of Ni at 44.5°, 56.7° and 76.3° for 2θ, corresponding to the dominant planes of metallic nickel (111), (200) and (220), respectively, with the JCPDS no. 04-850. The XRD patterns of Ni metal in Ni-loaded lignite char catalysts in this study also correspond to the report by Chaiklangmuang *et al.*[18]

The occurrences of Ni metals on all catalysts could be explained by the fact that the Ni ions (Ni^{2+}) that were exchanged with the oxygen-containing functional groups (*e.g.*, hydroxyl, carboxyl and metal-carboxylate groups) in the untreated coal and each treated coal were reduced by H_2 and CO and turned into Ni metal (Ni^0).[49,50] The H_2 and CO were generated by the decomposition of the aliphatic hydrocarbons, hydroxyl and carboxylate groups of Ni-loaded coal samples during pyrolysis at 650 °C.[51,52] The decomposition of the aliphatic hydrocarbons, hydroxyl and carboxylate groups of Ni-loaded lignite coal samples were confirmed by the FTIR spectra of catalysts. In Fig. 9, the IR bands of aliphatic hydrocarbons and oxygen-containing functional groups such as hydroxyl and carboxylate groups are not shown in the FTIR spectra of the catalysts.

Possible predictions of the chemical pathways for the preparation of Ni-loaded lignite char catalysts using MM coal supports are shown in Fig. 12. In the Ni ion exchange stage, most of the Ni ions were able to exchange with hydroxyl and metal-carboxyl groups in the form of $Ni(NH_3)_6^{2+}$ ions on the untreated coals and those modified by acid, alkali and alkali followed by acid treatments. After the pyrolysis process, coals were transformed into char catalysts. Meanwhile, NH_3 was released from $Ni(NH_3)_6^{2+}$ and then Ni metal (Ni^0) was formed *via* the reduction of Ni ions (Ni^{2+}) by H_2 and CO, which were produced during pyrolysis. Ni metal formed the active sites on catalysts that could promote catalytic reactions and control the product selectivity. The structure–activity relationship of the Ni loading mechanism of the catalyst is presented in Fig. 13.

The Ni element contained in the catalysts (Table 8) was in the range of 16.51–20.09 wt%, which depended on the preparation methods of Ni-loaded lignite char catalyst. Compared with the Ni/MMchar catalyst, the Ni/NaMMchar catalyst showed the highest Ni content of 20.09 ± 0.59 wt% because NaOH was a strong oxidant. The NaOH solution could have affected the increase in the number of oxygen-containing functional groups in MM coal such as –OH groups, which were sites for ion exchange. According to Herviyanti *et al.*,[35] NaOH treatment could increase the concentration of –OH groups in sub-bituminous coal since NaOH is an alkaline compound that could donate OH^- ions to sub-bituminous coal, which increased the cation exchange capacity of the coal. In the coal treatment with acetic acid, the Ni contents in Ni/AceMMchar and Ni/NaAceMMchar were 17.01 ± 0.19 wt% and 17.32 ± 0.23 wt%, respectively. When considered with Ni/MM char, the Ni contents of Ni/AceMMchar and Ni/NaAceMMchar increased since the acetic acid containing the carboxylic functional groups was able to be absorbed into the coal, which caused an increase in the content of carboxylic functional groups on the surface of the coal. Radenovic and Malina[14] reported that carbon black modification by the absorption of acetic acid onto carbon black could increase the nickel adsorption capacity from the solution due to the increase in the carboxylic functional group content on carbon black. The higher content of carboxylic functional groups could improve the adsorption of metal ions since the affinity between metals and carboxylic functional groups was extremely high.[53,54] The cases of Ni/HClMMchar and

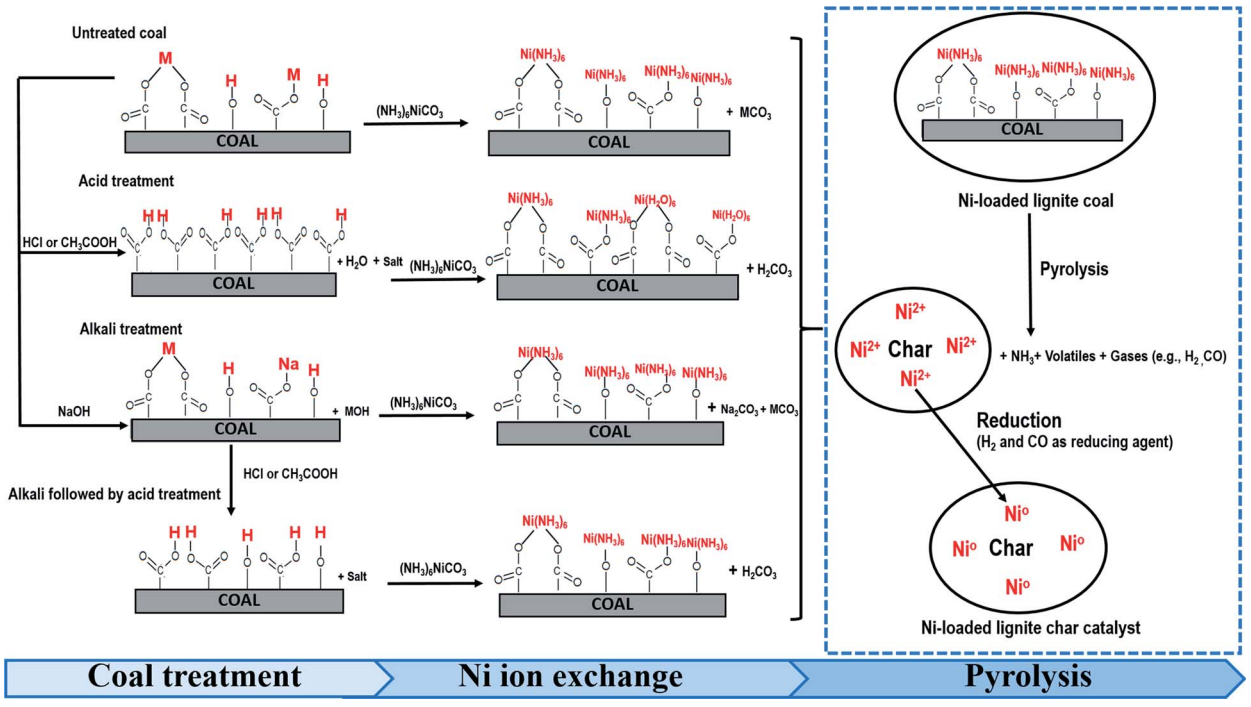

Fig. 12 Predicted chemical pathways for the preparation of Ni-loaded lignite char catalysts in this paper.

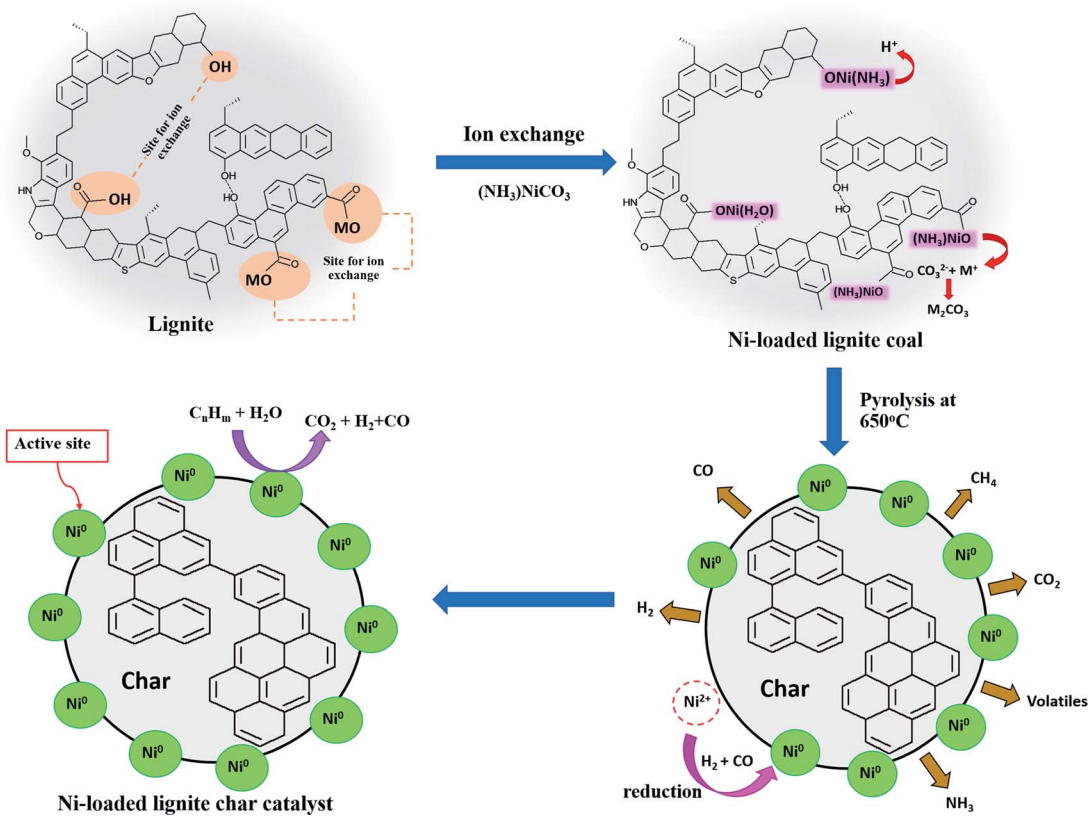

Fig. 13 Structure activity relationship of the Ni loading mechanism of the catalyst.

Table 8 Ni content in the catalysts

Catalyst	Ni content (wt%) ±SD
Ni/MMchar	16.55 ± 0.63
Ni/HClMMchar	16.62 ± 0.97
Ni/AceMMchar	17.01 ± 0.19
Ni/NaMMchar	20.09 ± 0.59
Ni/NaHClMMchar	16.51 ± 0.46
Ni/NaAceMMchar	17.32 ± 0.23

Ni/NaHClMMchar showed 16.62 ± 0.97 wt% and 16.51 ± 0.46 wt% of Ni contents, respectively, which were negligible differences in comparison with Ni/MMchar. It may be inferred that the HCl solution did not affect the number of functional groups involved in the ion exchange with Ni. The results of Ni content in catalysts reflected that the type of chemical agents for the coal treatment affected the content of Ni loading in the catalyst, particularly the NaOH and CH_3COOH solutions that influenced the enhancement of the Ni contents in the catalysts.

3.5 Oxygen functional groups on the catalyst surfaces

It is well known that the O/C atomic ratio can reflect the number of oxygen functional groups on catalyst surfaces.[55–57] As described in Section 3.4, the oxygen functional groups are related to the Ni loading content of the catalysts. To investigate the oxygen functional groups on the catalyst surfaces, the O/C atomic ratios of catalysts were determined by SEM-EDS analysis as presented in Fig. 14.

In acid treatment, the O/C atomic ratios of Ni/HClMMchar and Ni/AceMMchar catalysts were 0.14 and 0.12, respectively. Both modified catalysts had lower O/C atomic ratios than the Ni/MMchar catalyst. As a result, it may be inferred that the number of oxygen functional groups on the modified catalysts decreased when considered with the Ni/MMchar catalyst. The

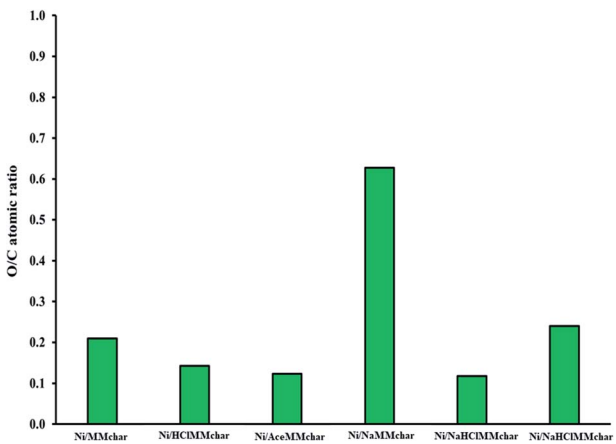

Fig. 14 O/C atomic ratios of catalysts.

reduction of O/C atomic ratios of the catalysts might be due to the elimination of carboxylate groups in the pyrolysis stage.

For the alkali treatment, the Ni/NaMMchar catalyst had the highest O/C atomic ratio at 0.63, corresponding to the highest Ni content as well. The enhancements of the O/C atomic ratio and Ni content catalyst were caused by the number of oxygen-containing functional groups on MM coal promoted by the NaOH solution.

In the treatment with alkali followed by acid, the O/C atomic ratios of Ni/NaHClMMchar and Ni/NaAceMMchar were 0.12 and 0.24, respectively. The increase in the O/C atomic ratio of Ni/NaAceMMchar occurred with the formation of carbonate compounds (CO_3^{2-}) in the catalyst as confirmed by FTTR results (Fig. 9). The appearance of carbonate compounds was also illustrated by the DTG results in Section 3.6 as presented in the next section.

(Fig. 15) shows the morphological studies and distributions of oxygen and nickel atoms on the surfaces of Ni/NaMMchar (Fig. 15a), Ni/AceMMchar (Fig. 15b) and Ni/NaAceMMchar (Fig. 15c) catalysts. Based on EDS-mapping images, the oxygen and nickel atoms had good dispersions on the catalyst surfaces. Focusing on the surface morphology of the catalysts, the surface of Ni/NaMMchar was smoother than those of Ni/AceMMchar and Ni/NaAceMMchar. This was because the NaOH treatment caused the coalescence of coal and the formation of sodium-aluminosilicate gel film that covered the catalyst surface[10] and as a result, the surface of Ni/NaMMchar was quite unruffled.

3.6 Thermal behaviour and stability of Ni-loaded lignite char catalysts

In view of the thermal behaviours of Ni-loaded lignite char catalysts under a nitrogen gas atmosphere, the DTG curves of the catalysts are presented in Fig. 16 and the maximum peak temperatures from DTG curves are listed in Table 9. The pyrolyzed temperature can be divided into four zones.

The DTG peaks of the catalysts were observed at around 27–150 °C in the first zone. The maximum peak temperatures occurred at about 48–62 °C, which resulted from the loss of moisture in the catalysts.[5] In the second zone at 150–450 °C, low weight-loss rates were observed in the range of 9–25 μg min^{-1} and all the fresh catalysts decomposed slowly.

The third zone clearly showed the DTG-decompositions of Ni/HClMMchar, Ni/AceMMchar and Ni/NaHClMMchar catalysts at temperatures ranging from 496 °C to 557 °C, 400 °C to

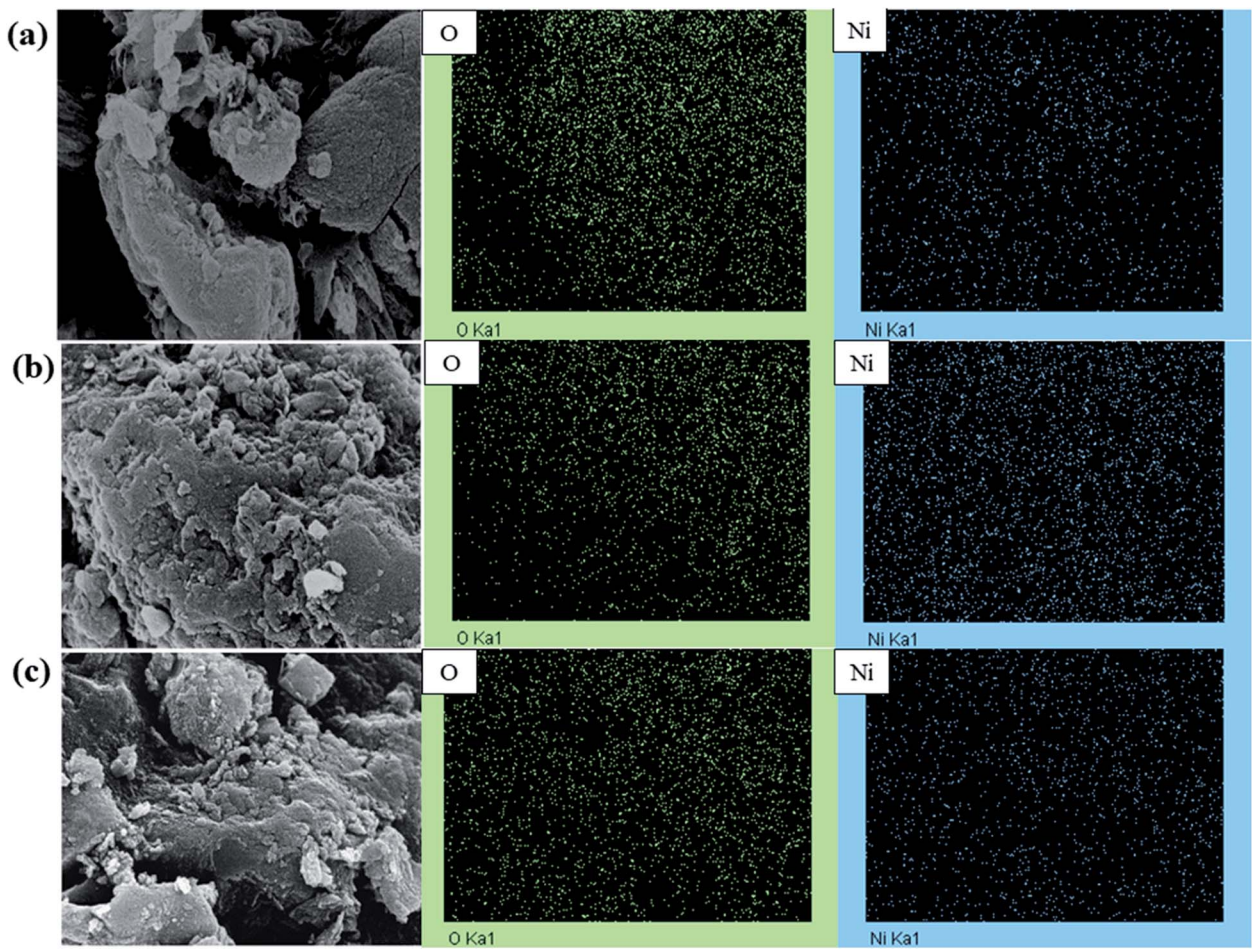

Fig. 15 SEM images and distributions of oxygen and nickel atoms on the catalyst surfaces: (a) Ni/NaMMchar, (b) Ni/AceMMchar and (c) Ni/NaAceMMchar.

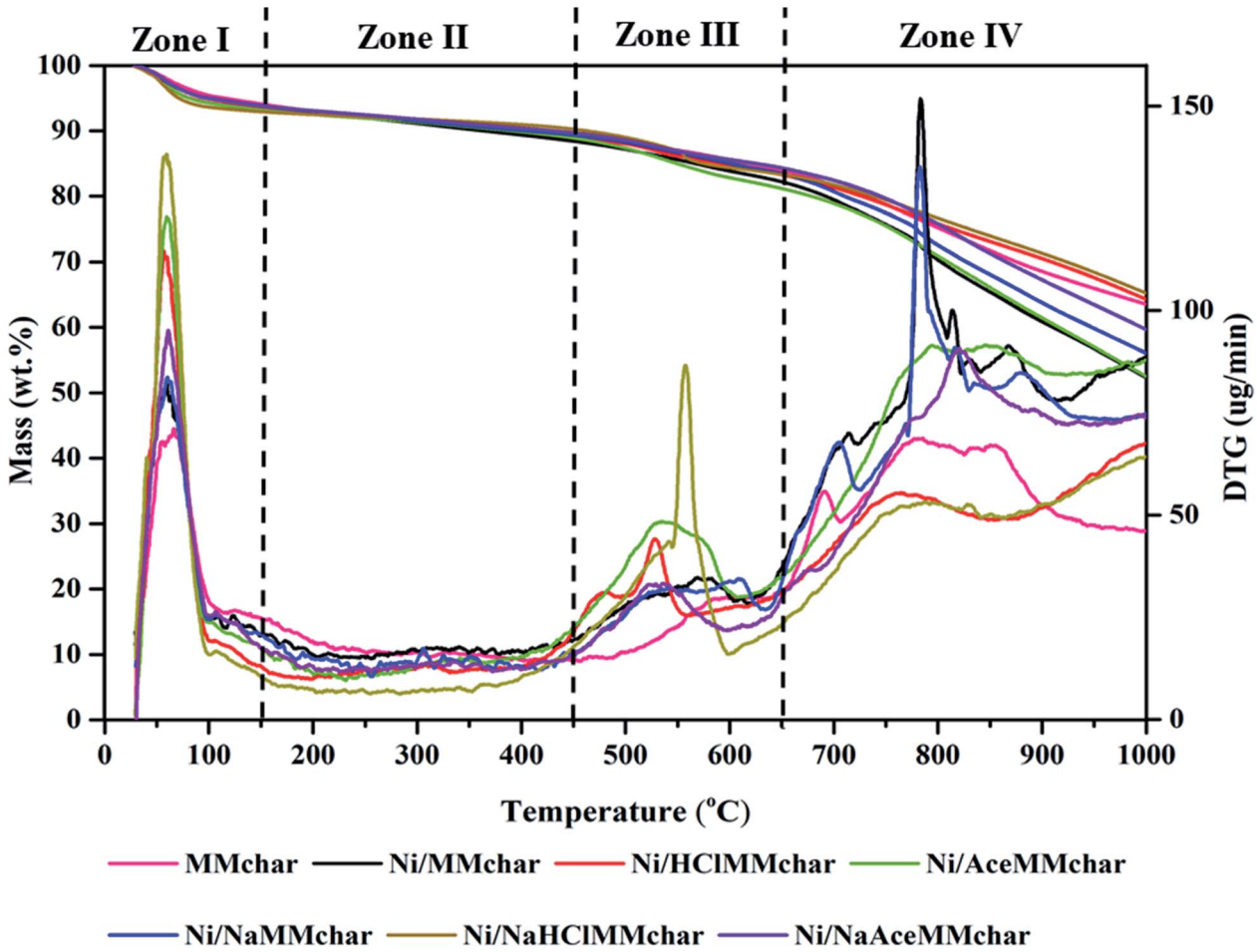

Fig. 16 TGA-DTG curves of fresh catalysts at 25–1000 °C.

Table 9 Maximum peak temperatures of the catalysts from DTG curves

	Maximum peak temperature (°C)		
Catalyst	First peak	Second peak	Third peak
Ni/MMchar	56	—	783
Ni/HClMMchar	48	530	—
Ni/AceMMchar	62	544	—
Ni/NaMMchar	58	—	763
Ni/NaHClMMchar	56	557	—
Ni/NaAceMMchar	50	—	820

603 °C, and 400 °C to 600 °C, respectively. Li *et al.*[58] investigated that the obvious weight loss at around 200–400 °C was due to the disaggregation, release of the volatiles, and decomposition of lignite. Cheng *et al.*[59] studied several coals treated with acids and reported that in the temperature range of 400–600 °C, the bonds between aliphatic carbons and between aliphatic carbon and aromatic carbon were cracked. Similarly, the decompositions of the Ni/lignite char catalysts were examined by DTG in this zone. The maximum peak temperatures of Ni/HClMMchar, Ni/AceMMchar and Ni/NaHClMMchar catalysts were 530 °C, 544 °C and 557 °C, respectively. According to Shi *et al.*,[60] the single peak at around 450 °C confirmed the assignment of aliphatic carbon bonds, where the cleavage of aromatic carbon and nitrogen bond peaked at 425 °C, and the breakage of aromatic carbon and aliphatic carbon bonds and aromatic carbon and oxygen bonds peaked at around 550 °C.

In the fourth zone, the apparent DTG peaks of Ni/MMchar, Ni/NaMMchar and Ni/NaAceMMchar catalysts were observed in the temperature range of 722–839 °C, 723–830 °C and 685–882 °C, respectively. According to Li *et al.*,[58] the temperature range of 720–920 °C corresponds to the loss of minerals in lignite that were mainly carbonate compounds in coals. Li *et al.*[61] investigated the thermal analysis of the calcium carbonate decomposition, and they reported the initial temperature of $CaCO_3$ at 600 °C and the final temperature at 829 °C, and its maximum peak temperature was 793 °C. Therefore, the apparent peaks in zone IV of this research implied the decomposition of carbonate compounds. From the FTIR spectra in Fig. 9, we also found the forms of carbonate compounds. According to the XRD patterns in Fig. 10, these carbonate compounds should be $CaCO_3$ and Na_2CO_3 since their

Table 10 Comparison of Ni-loaded lignite char catalysts and other Ni-loaded heterogeneous catalysts

Application	Fuel	Catalyst	Condition	Result	Ref.
Biomass gasification	Japanese cypress	14.7 wt% Ni/YL and 20 wt% Ni/Al_2O_3	Two-stage fixed bed reactor operated at 650 °C under N_2 atmosphere	-Compared with non-catalyst, the total gas yields increased by 2.5 times with Ni/Al_2O_3 and 3.3 times with Ni/LY -The Ni/LY could produce more gas than Ni/Al_2O_3	2
Catalytic gasification	Waste biomass (wood chip of red pine and pig manure compost)	Ni/BBC and Ni/Al_2O_3	Two-stage fixed bed reactor operated at 650 °C under N_2 atmosphere	Compared with non-catalyst, the gas yields of H_2 and CO increased dramatically in the presence of Ni catalysts, with the total gas yield of 2.9 times in Ni/Al_2O_3 and 3.1 times in Ni/BCC	3
Biomass gasification	Red pine and Japanese cedar	9 wt% Ni/YL and 20 wt% Ni/Al_2O_3	Fluidized bed gasifier operated at 650 °C under N_2 atmosphere	-Ni/YL could produce more H_2 and CO than Ni/Al_2O_3 -The surface areas of Ni/YL before and after use were higher than Ni/Al_2O_3 -The surface areas of Ni/YL and Ni/Al_2O_3 before use were 350 and 104 $m^2 s^{-1}$, respectively -The surface areas of Ni/YL and Ni/Al_2O_3 after use were 339 and 32 $m^2 s^{-1}$, respectively	65
Catalytic reforming	Toluene	19 wt% Ni/LY and 20 wt% Ni/Al_2O_3	Reforming of toluene at 650 °C under N_2 atmosphere	-Ni/LY was a potential anti-coke catalyst -Ni/Al_2O_3 was not a stable catalyst and high carbon disposition	66

melting points are 825 °C and 580 °C, respectively. In this study, the Ca and Na elements were present high percentages as mentioned in Table 3.

Mostly, the Ni/lignite char catalysts have been applied in the thermo-chemical processes such as pyrolysis,[62–64] gasification[2,3,5,6,17,65] and reforming.[66] The predictions of thermal stabilities of the catalysts were important to inspect the selection of catalyst applications.

As seen in Fig. 16, the TGA results indicated the loss of moisture in the range of 4.95–6.38 wt%. Generally, the released moisture from the catalyst affected the amount of steam in order to interfere with the catalytic reaction. According to the literature reviews,[2–5] steam was one of the factors that was influential in the tar decomposition for producing hydrogen-rich gas. The slower mass loss was the pheromone in the second zone and the mass loss percentages were in the range of 2.69–5.35 wt%. For the third zone, the mass loss percentages of all fresh catalysts were in the range of 5.37–6.25 wt%. The low mass loss in zones I and III indicated that the temperature in the range of 150–650 °C hardly affected the thermal stabilities of catalysts. At higher temperatures, the mass loss percentages of catalysts in the fourth zone drastically increased, which were in the range of 18.18–29.92 wt%. The mass loss percentages of catalysts in descending order were Ni/AceMMchar > Ni/MMchar > Ni/NaMMchar > Ni/NaAceMMchar > Ni/HClMMchar > Ni/NaHClMMchar.

The comparisons of Ni-loaded lignite char catalysts with other Ni-loaded heterogeneous catalysts are presented in Table 10. The advantages of Ni/lignite char catalysts are more predominant than other Ni-loaded heterogeneous catalysts and may be summarized thus: (i) their catalyst surfaces are high and stable, indicating the increasing catalytic activity; (ii) the catalysts have higher efficiency in gas production; (iii) carbon depositions on catalysts are lower, resulting in the reduction of catalyst deactivation.

4. Conclusions

This study focused on the influence of acid, alkali and alkali followed by acid treatments on lignite coal properties and their implications during the synthesis of Ni/lignite char catalyst *via* ion exchange. The Ni loading mechanisms were studied through FTIR, XRD, AAS and SEM-EDS including TGA-DTG for thermal behaviours. Ni loaded on original coal and treated coals were pyrolyzed at 650 °C to produce the six samples of Ni-loaded lignite char catalysts, which were Ni/MMchar, Ni/HClMMchar, Ni/AceMMchar, Ni/NaMMchar, Ni/NaHClMMchar and Ni/NaAceMMchar catalysts. The results found that the differences in coal treatments remarkably influenced ash contents and the functional groups in coals. The decreases in ash contents of HClMM, AceMM, NaHClMM and NaAceMM coals indicated that the exchangeable metallic species were removed

by transforming metal-carboxylates into carboxyl groups. The transformations of metal-carboxylates were confirmed by the increased $\Delta\vartheta(COO^-)$ value. In terms of the Ni loading mechanism into coal, the carboxyl groups on acid-treated coals connected with Ni ions in the form of metal-carboxylate. For alkali treatment, hydroxyl and metal-carboxylate groups were sites for the Ni ion exchange, likewise original coal. For the treatment involving alkali followed by acid, the ion exchange of Ni ions on NaHClMM and NaAceMM coals occurred through hydroxyl and carboxyl groups; besides, the Ni ion exchange with metal-carboxylates was observed on NaAceMM coal. Considering the Ni ion forms, the $Ni(NH_3)_6^{2+}$ ion form was detected on MM, AceMM, NaMM, NaHClMM and NaAceMM coals, while the $Ni(NH_3)_6^{2+}$ and $Ni(H_2O)_6^{2+}$ ions were found on HClMM coal. In the production of Ni-loaded lignite char catalysts, the different Ni contents in catalysts emerged from the chemical agent types used in coal treatment. NaOH and CH_3COOH solutions could modify the functional groups in coal in order to promote hydroxyl and carboxylic groups, resulting in a higher Ni loading capacity in catalysts. Therefore, the changes in the functional groups in the treated coals were the key factors in controlling the Ni loading on coals. Finally, the author expects that this study will shed light on the development of the metal-loaded char catalyst that can be applied in the conversion processes such as fuel upgrading and alternative energy from biomass transformation.

Conflicts of interest

There are no conflicts to declare.

Acknowledgements

This research project is supported by TSRI. In addition, this research work is partially supported by Chiang Mai University. The authors would like to acknowledge Electricity Generating Authority of Thailand and Department of Industrial Chemistry, Faculty of Science, Chiang Mai University.

Notes and references

1 J. I. Hayashi and C. Z. Li, *Advances in the science of Victorian brown coal*, 2004, pp. 11–84, DOI: 10.1016/B978-008044269-3/50003-0.
2 L. Li, K. Morishita, H. Mogi, K. Yamasaki and T. Takarada, *Fuel Process. Technol.*, 2010, **91**, 889–894.
3 X. Xiao, J. Cao, X. Meng, D. Le, L. Li, Y. Ogawa and T. Takarada, *Fuel*, 2013, **103**, 135–140.
4 S. Kim, D. Chun, Y. Rhim, J. Lim, S. Kim, H. Choi and J. Yoo, *Int. J. Hydrogen Energy*, 2015, **40**, 11855–11862.
5 B. S. Wang, J. P. Cao, X. Y Zhao, Y. Bian, C. Song, Y. P. Zhao and T. Takarada, *Fuel Process. Technol.*, 2015, **136**, 17–24.
6 C. Phuhiran, T. Takarada and S. Chaiklangmuang, *Int. J. Hydrogen Energy*, 2014, **39**, 3649–3656.
7 S. Aich, D. Behera, B. K. Nandi and S. Bhattacharya, *Int. J. Coal Sci. Technol.*, 2020, **7**, 766–777.
8 W. Li, Z. Q. Bai, J. Bai and X. Li, *Fuel*, 2017, **197**, 209–216.
9 S. K. Behera, U. Kumari and B. C. Meikap, *J. Min. Metall., Sect. A*, 2018, **54**, 1–24.
10 S. K. Behera, S. Chakraborty and B. C. Meikap, *Fuel*, 2017, **196**, 102–109.
11 H. Dhawan and D. K. Sharma, *Int. J. Coal Sci. Technol.*, 2019, **6**, 169–183.
12 J. Starck, P. Burg, D. Cagniant, J. M. Tascón and A. Martinez-Alonso, *Fuel*, 2004, **83**, 845–850.
13 J. Ren, J. P. Cao, X. Y. Zhao, F. Wei, T. L. Liu, X. Fan and X. Y. Wei, *Fuel*, 2017, **202**, 345–351.
14 A. Radenovic and J. Malina, *Hem. Ind.*, 2013, **67**, 51–58.
15 S. S. Shah, I. Ahmad, W. Ahmad, M. Ishaq and H. Khan, *Energy Fuels*, 2017, **31**, 7867–7873.
16 S. Mukherjee, *Energy Fuels*, 2003, **17**, 559–564.
17 L. Feng, X. Liu, L. Song, X. Wang, Y. Zhang, T. Cui and H. Tang, *Powder Technol.*, 2013, **247**, 19–23.
18 S. Chaiklangmuang, L. Li, N. Kannari and T. Takarada, *J. Energy Inst.*, 2018, **91**, 222–232.
19 N. Duongbia, N. Kannari, K. Sato, T. Takarada and S. Chaiklangmuang, *Alexandria Eng. J.*, 2021, In press.
20 T. Ronnachai, C. Chatchwan, and C. Suparin, *The 21st international union of materials research societies-international conference in asia*, 2020, p. 392.
21 F. Rehman, S. W. Ahmad, M. S. Zafar, S. Ahmad and M. Zia-Ul-Haq, *Pol. J. Chem. Technol.*, 2018, **20**, 103–109.
22 M. Kumar and R. H. Shankar, *Energy Sources*, 2000, **22**, 187–196.
23 K. Kaneko, L. Li, A. Matsushima, H. Sato, T. Shimizu, H. Kim and T. Takarada, *J. Chem. Eng. Jpn.*, 2016, **49**, 294–299.
24 C. R. Ward, *Int. J. Coal Geol.*, 2002, **50**, 135–168.
25 C. R. Ward, *Int. J. Coal Geol.*, 1991, **17**, 69–93.
26 S. D. Barma, R. Sathish and P. K. Baskey, *J. Cleaner Prod.*, 2018, **195**, 1203–1213.
27 K. M. Steel, J. Besida, T. A. O'Donnell and D. G. Wood, *Fuel Process. Technol.*, 2001, **70**, 171–192.
28 B. Manoj and P. Narayanan, *J. Miner. Mater. Charact. Eng.*, 2013, **1**, 39–43.
29 W. Cheng, J. Xue, J. Xie, G. Zhou and W. Nie, *Energy Fuels*, 2017, **31**, 13834–13841.
30 L. Ma, R. Guo, Y. Gao, L. Ren, G. Wei and C. Li, *Combust. Sci. Technol.*, 2019, **191**, 1456–1472.
31 B. D. Nandiyanto, R. Oktiani and R. Ragadhita, *Indonesian Journal of Science and Technology*, 2019, **4**, 97–118.
32 E. G. Palacios, G. Juárez-López and A. J. Monhemius, *Hydrometallurgy*, 2004, **72**, 139–148.
33 S. K. Papageorgiou, E. P. Kouvelos, E. P. Favvas, A. A. Sapalidis, G. E. Romanos and F. K. Katsaros, *Carbohydr. Res.*, 2010, **345**, 469–473.
34 Y. Ban, Y. Wang, N. Li, R. He, K. Zhi and Q. Liu, *R. Soc. Open Sci.*, 2018, **5**, 180717–180727.
35 H. Herviyanti, T. B. Prasetyo, J. Juniarti, S. Prima and S. Wahyuni, *International Journal on Advanced Science, Engineering and Information Technology*, 2018, **8**, 2052–2058.
36 A. Sarkar, D. Seth, M. Jiang, F. T. Ng and G. L. Rempel, *Top. Catal.*, 2014, **57**, 730–740.
37 Z. Kledyński, A. Machowska, B. Pacewska and I. Wilińska, *J. Therm. Anal. Calorim.*, 2017, **130**, 351–363.

38 D. P. Domonov, S. I. Pechenyuk, A. T. Belyaevskii and K. V. Yusenko, *Nanomaterials*, 2020, **10**, 389–399.
39 R. A. Nyquist and R. O. Kagel, *Handbook of infrared and Raman spectra of inorganic compounds and organic salts*, Academic press, 2012, DOI: 10.1002/9780470027325.s4104.
40 A. Sharma, H. Nakagawa and K. Miura, *Fuel*, 2006, **85**, 2396–2401.
41 J. P. Cao, T. L. Liu, J. Ren, X. Y. Zhao, Y. Wu, J. X. Wang and X. Y. Wei, *J. Anal. Appl. Pyrolysis*, 2017, **127**, 82–90.
42 Y. Shinohara and N. Tsubouchi, *ACS Omega*, 2020, **5**, 1688–1697.
43 N. Tsubouchi, Y. Mochizuki, Y. Shinohara, Y. Hanaoka, T. Kikuchi and Y. Ohtsuka, *Energy Fuels*, 2018, **32**, 226–232.
44 X. Li, L. Fan, G. G. Wu, Z. Q. Bai and W Li, *Anal. Lett*, 2018, **51**, 2532–2543.
45 J. M. Whittinghill, J. Norton and A. Proctor, *J. Am. Oil Chem. Soc.*, 1999, **76**, 1393–1398.
46 P. K. Singh, P. K. Rajak, M. P. Singh, V. K. Singh and A. S. Naik, *Int. J. Coal Sci. Technol.*, 2016, **3**, 104–122.
47 J. Liang, Y. Z. Wang, C. C. Wang and S. Y. Lu, *J. Matter. Chem. A.*, 2016, **4**, 9797–9806.
48 T. Hatori, K. Morishita, N. Kannari and T. Takarada, *J. Jpn. Inst. Energy*, 2017, **96**, 519–524.
49 T. Hatori, K. Morishita, N. Kannari and T. Takarada, *J. Jpn. Inst. Energy*, 2017, **96**, 139–143.
50 Z. Na, Z. Xu, L. Ziliang, L. Qiuxiang, L. Wei, C. Qiue and Y. Shenfu, *Asia-Pac. J. Chem. Eng.*, 2020, **15**, 2384–2395.
51 T. Xu, S. C. Srivatsa and S. Bhattacharya, *J. Anal. Appl. Pyrolysis*, 2016, **122**, 122–130.
52 L. Zhang, S. Qi, N. Takeda, S. Kudo, J. Hayashi and K. Norinaga, *Int. J. Coal Sci. Technol.*, 2018, **5**, 452–463.
53 J. P. Chen, S. Wu and K. H. Chong, *Carbon*, 2003, **41**, 1979–1986.
54 D. Mugisidi, A. Ranaldo, J. W. Soedarsono and M. Hikam, *Carbon*, 2007, **45**, 1081–1084.
55 G. Zhou, C. Xu, W. Cheng, Q. Zhang and W. Nie, *J. Anal. Methods Chem.*, 2015, **2015**, 1–8.
56 X. Ma, B. Zhou, A. Budai, A. Jeng, X. Hao, D. Wei and D. Rasse, *Analysis*, 2016, **47**, 593–601.
57 S. Bakshi, C. Banik and D. A. Laird, *Chemosphere*, 2018, **194**, 247–255.
58 L. Li, X. Wang, S. Wang, Z. Cao, Z. Wu, H. Wang and J. Liu, *Electroanalysis*, 2016, **28**, 243–248.
59 X. Cheng, L. Shi, Q. Liu and Z. Liu, *Energy Fuels*, 2019, **33**, 2008–2017.
60 L. Shi, Q. Liu, X. Guo, W. Wu and Z. Liu, *Fuel Process. Technol.*, 2013, **108**, 125–132.
61 X. G. Li, Y. Lv, B. G. Ma, W. Q. Wang and S. W. Jian, *Arabian J. Chem.*, 2017, **10**, S2534–S2538.
62 Z. Lei, S. Hao, J. Yang and X. Dan, *Int. J. Hydrogen Energy*, 2020, **45**, 19280–19290.
63 C. Li, C. Zhang, M. Gholizadeh and X. Hu, *J. Hazard. Mater.*, 2020, **399**, 123075–123085.
64 L. Chao, C. Zhang, L. Zhang, M. Gholizadeh and X. Hu, *Waste Manag.*, 2020, **116**, 9–21.
65 D. D. Le, X. Xiao, K. Morishita and T. Takarada, *J. Chem. Eng. Jpn.*, 2009, **42**, 51–57.
66 J. P. Cao, J. Ren, X. Y. Zhao, X. Y. Wei and T. Takarada, *Fuel*, 2018, **217**, 515–521.